Science of the Total Environment 951 (2024) 175250

Contents lists available at ScienceDirect

Science of the Total Environment

journal homepage: www.elsevier.com/locate/scitotenv

Nitrate trend reversal in Dutch dual-permeability chalk springs, evaluated by tritium-based groundwater travel time distributions

Hans Peter Broers[a,*], Mariëlle van Vliet[a], Tano Kivits[a], Ronald Vernes[a], Timo Brussée[b], Jürgen Sültenfuß[c], Dico Fraters[b]

[a] TNO Geological Survey of the Netherlands, P.O. Box 80015, 3508 TA Utrecht, the Netherlands
[b] National Institute of Public Health and the Environment, Bilthoven, the Netherlands
[c] University of Bremen, Institute of Environmental Physics, Department of Oceanography, Bremen, Germany

HIGHLIGHTS

- 90 Springs show diverging, sometimes multi-modal, travel time distributions (TTDs).
- Nitrate responses of springs following N-input reductions depend on their TTDs.
- Models and measurements of 90 springs point to clear nitrate trend reversals.
- TTDs influence peak concentrations, lag times and steepness of declines.
- Large young water fractions favor high nitrate peaks and steep post-reversal declines.

GRAPHICAL ABSTRACT

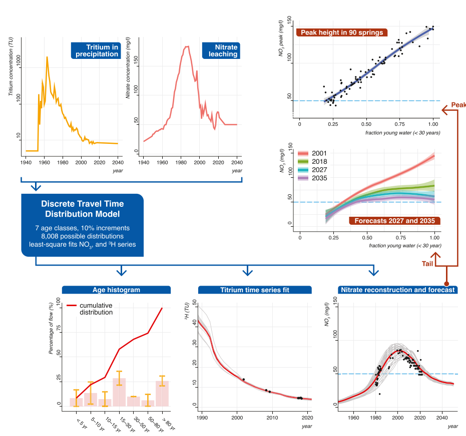

ARTICLE INFO

Editor: Christian Herrera

Keywords:
Groundwater age distribution
Nitrate trend reversal
Measures to reduce nitrogen inputs
Time lag
Nitrate legacy
Young water fraction

ABSTRACT

Historical use of fertilizer and manure on farmlands is known to have a lasting impact on ecosystems and water resources, but few studies assess the legacy of nitrate pollution on groundwater and surface water after farming applications were reduced. We studied the response of nitrate in spring water to a reduction of nitrogen fertilizer applications in agriculture realized since the mid-1980s. We assessed the travel time distribution of groundwater based on a time series of tritium measurements for 90 springs and small brooks that drain a dual porosity chalk aquifer. The travel time distributions were constrained using the tritium data in combination with time series of nitrate concentrations, applying a shape-free travel time distribution model. A clear trend reversal of nitrate concentrations was observed and simulated for springs with a large fraction of young water (< 30 years old) whereas the nitrate response in springs with relatively older water was attenuated and delayed. We conclude that obtaining a time series of tritium data helps to constrain age distributions of water that is discharged from dual permeability aquifers. The fraction of water aged <30 years was a meaningful parameter to distinguish between different types of springs. Nitrate trends in springs that drain large fractions of young water (> 0.6) show higher

* Corresponding author.
E-mail address: hans-peter.broers@tno.nl (H.P. Broers).

https://doi.org/10.1016/j.scitotenv.2024.175250
Received 2 May 2024; Received in revised form 30 July 2024; Accepted 1 August 2024
Available online 9 August 2024

peak concentrations, shorter lag-time between leaching and outflow peaks and steeper declines after trend reversal, relative to trends in springs which are dominantly fed by older groundwater. The study thus shows that the nitrate legacy of groundwater systems is strongly determined by the range of their travel time distributions, and trend reversal in receiving springs and surface waters may appear within 10 to 15 years after measures to reduce nitrate losses from farming.

Secondary keywords

Tritium, Trends, Reaction time, Natural springs, Chalk, Dual permeability, Nitrogen leaching, Water quality standards, Compliance

1. Introduction

Historical use of fertilizer and manure on farmlands is known to have a lasting impact on ecosystems and water resources, but few studies quantify the legacy of nitrate pollution on groundwater and surface water after farming applications were reduced (Visser et al., 2007, 2009; Hansen et al., 2010; Van der Velde et al., 2010; Kaandorp et al., 2021). It is generally recognized that past farming practices may have left a legacy of nitrate pollution in the environment, even if current fertilizer applications are reduced (e.g., Böhlke, 2002; Visser et al., 2007; Van Meter et al., 2016; Kaandorp et al., 2021; Sarrazin et al., 2022; Dessirier et al., 2023; Golden et al., 2023). Most existing studies rely on modeling approaches at the scale of large river catchments and often lack sufficient and adequate monitoring data to assess biogeochemical and hydrological nitrogen legacies. With the exception of Kaandorp et al. (2021), few studies utilize age tracers to quantify travel time distributions (TTD) in the subsurface which determine the hydrological legacy, thus making it one of the most uncertain variables in assessing surface water nitrogen legacies (e.g., Sarrazin et al., 2022). However, groundwater age dating has successfully been applied in unraveling nitrate trends and legacies for groundwater abstractions, providing independent information about the hydrological regimes in addition to the measured nitrate data (e.g., Visser et al., 2013; Alikhani et al., 2016; Visser et al., 2016; Tesoriero et al., 2019). We investigated the response of nitrate in spring water to a reduction in the use of nitrogen fertilizers in agriculture in the south of the Netherlands realized since the mid-1980s and assessed the travel time distribution of groundwater based on a time series of tritium measurements for 90 springs and small brooks that drain a dual porosity aquifer, which consists of soft limestones known as 'chalk' in western Europe.

The Netherlands serves as an ideal testing ground, because of its intensive farming systems with increasing inputs of nitrogen fertilizers after the Second World War in combination with national and EU regulations that led to a strong reduction in nitrogen use since around 1985 (e.g., Van Grinsven et al., 2012). The Netherlands holds one of the most intensive farming systems worldwide, which has significantly impacted groundwater resources (e.g., Boumans et al., 2008; Visser et al., 2007; Post et al., 2020; Mendizabal and Stuyfzand, 2011; Mendizabal et al., 2012; Broers et al., 2021; Spijker et al., 2021). Leaching of fertilizers, manure, pesticides and veterinary antibiotics has affected the quality of groundwater (Tiktak et al., 2002; Visser et al., 2007; Schipper et al., 2008; Sjerps et al., 2019; Kivits et al., 2018). Awareness of the negative consequences of excess nitrogen, leaching as nitrate into groundwater, began in the early 1980's (e.g., Duijvenbooden and Waegeningh, 1987) and resulted in the Netherlands Manure and Fertilizer Act in 1985 which implemented regulations to reduce the environmental impact of livestock farming by preventing the growth of livestock production and by reducing manure production and use. Excessive use of animal manure has since been regulated by application standards. Additional regulations were included after the EU Nitrates Directive 91/676/EC came into force in 1991 (EU Commission, 1991), which sets a standard of 50 mg/l nitrate in groundwater. The Nitrates Directive obliges all Member States to implement Nitrate Action Programmes, restricting the application of fertilizer and manure, and to evaluate these programmes every four years (e.g., Oenema et al., 1998; Van Grinsven et al., 2012). To monitor the effectiveness of these action programmes, management at a selection of about 450 farms is registered and the quality of water leaching from the rootzone of their fields is determined in the uppermost groundwater one to four times per year (Fraters et al., 1998, 2021; Van Duijnen et al., 2021).

In the southernmost part of the Netherlands, Zuid-Limburg (Fig. 1), the groundwater level at elevated loess plateaus occurs at relatively large depth (tens of meters). In these areas, soil moisture was extracted from below-rootzone soil samples to monitor the quality of the rootzone leachate in this region (Fraters et al., 2017, 2023). The monitoring results showed that nitrate concentrations in rootzone leachate decreased since the mid-nineties till 2011 and, thereafter, varied on average around 75 mg/l (Fraters et al., 2021; see Section 2.3.2 for details). Thus, the nitrate concentration in the leachate exceeded the Nitrates Directive threshold of 50 mg/l; however, this threshold applies to groundwater and not to soil moisture.

In addition, the water of springs that drain the loess plateaus was sampled every six to eight years to study the long-term effect of the minerals policy on groundwater and surface water in this region. These springs naturally drain the groundwater systems in this region and function as the outlets of the aquifer system. The nitrate concentrations at the springs are tested against the compliance regime of the EU Nitrates Directive (91/676/EC) and the EU Groundwater Directive (2006/118/EC), which both set a groundwater quality standard of 50 mg/l. Moreover, water that discharges at the springs feeds the regional system of brooks for which surface water quality standards and ecological objectives apply, following the EU Water Framework Directive (2000/60/EC). Thus, measurements in spring water were meant to assess whether the concentrations in the rootzone leachate threatens groundwater quality or may result in exceedance of thresholds for ecological objectives of the receiving surface waters and associated terrestrial and aquatic ecosystems (e.g., De Mars et al., 2024). As such, the combined measured nitrate concentrations at both the inlet of the groundwater system (below-rootzone soil moisture concentrations at the loess plateaus) and the outlets of the system (the springs) provide information on the effectiveness of Dutch manure policy in this region. Compared to studies focusing on large catchments and incorporating complex modeling frameworks that consider root zone denitrification, accumulation processes, surface water retention, and additional anthropogenic point sources in receiving surface waters (e.g., Sarrazin et al., 2022; Dessirier et al., 2023), our study offers the advantage of directly examining spring water at the immediate outlets of the groundwater system. This is achieved through a measured time series of nitrate leached below the root zone of the farmlands, thereby circumventing the need to incorporate the aforementioned processes in the evaluation.

Based on previous work by Osenbrück et al. (2006), Van der Velde et al. (2010) and Kaandorp et al. (2018, 2021), we hypothesized that the travel time distribution (TTD) is a prime factor determining the nitrate response of the groundwater system we studied. The TTD summarizes the transit times for a mixture of groundwater flow paths, each with a respective travel time, and is evaluated at the point of groundwater discharge, which in our case corresponds to the springs that drain the loess plateaus (e.g., Solder et al., 2016; Osenbrück et al., 2006). A travel time distribution is typically derived using a set of multiple age tracers measured at a specific sampling time (e.g., Osenbrück et al., 2006; Katz et al., 2001; Eberts et al., 2012; Visser et al., 2013; Massoudieh et al., 2014; McCallum et al., 2017; Broers et al., 2021) and is typically evaluated with a lumped parameter model assuming a specific form of distribution which integrates dispersion, diffusion and mixing along and between discrete groundwater flow paths (e.g., Maloszewski and Zuber, 1982, 1993, 1998; Jurgens et al., 2012, 2016; Osenbrück et al., 2006; Suckow, 2012). Alternatively, shape-free models may be applied, which enable free forms of travel time distribution without specifying a predefined distribution (e.g., Visser et al., 2013; Alikhani et al., 2016; McCallum et al., 2017; Broers et al., 2021; Rädle et al., 2022). The advantage of the latter type of models is that they allow for multi-modal travel time distributions, which seemed appropriate for our groundwater system that is supposedly determined by dual porosity flow including diffuse matrix flow and conduit-controlled flow (Van Rooijen, 1993; Quinlan and Ewers, 1985; Mull et al., 1988; Kuniansky et al., 2023). Instead of sampling multiple tracers at one specific moment in time, we sampled one specific tracer (tritium) at different moments in time, following previous examples by Stolp et al. (2010) and Suckow et al. (2013) for the Fischa-Dagnitz spring system in Austria. This approach was more feasible because initial tests in 2008 showed that degassing just before or during sampling affected the gas samples that were collected at the spring outlets. Low-frequency tritium sampling was therefore considered to be more robust, with the disadvantage of collecting a low-resolution time series over a period of about 18 years (2001–2018) to find a meaningful decrease of tritium concentrations over time to be tested against the convoluted tracer concentration of the TTD models.

Thus, for our aim to improve the understanding of the nitrate evolution and forecast future developments, we used the time series of tritium and nitrate to quantify the travel time distributions (TTD) of the springs, acknowledging the dual permeability characteristics of the chalk aquifer. Here, we hypothesized that the nitrate response to measures aimed at reducing the leaching of nitrate to groundwater depends strongly on the travel times of water and contaminants towards the springs that drain the loess plateaus in the south of the Netherlands. The studied system is particularly relevant for studying the legacy of nitrate, because the groundwater system was loaded with nitrate over a time span of about 50 years, with a sharp decline of nitrogen use in agriculture since 1985, that resulted from the robust measures taken to reduce nitrogen loss from agricultural fields, following the implementation of Dutch and EU legislation.

2. Material and methods

2.1. Study area and hydrogeological setting

2.1.1. Topography and climate

Zuid-Limburg, in the south of the Dutch province of Limburg, is part of the Meuse River catchment (Fig. 1). The area features hilly terrain with elevations from 45 to 50 m + MSL near the Meuse River to 320 m + MSL in the southeast, and shallow presence of soft limestones. It consists of "loess plateaus" with altitudes between 100 and 250 m, and brook valleys below 100 m + MSL. Fertile loess soils support arable and dairy farming, as well as fruit growing. The region's brooks are fed by small springs which often have concentrations above the 50 mg/l threshold of the EU Nitrate and Groundwater Directives (Fig. 1). High nitrate levels are also found in groundwater, affecting water supplies and nature reserves (Van Lanen et al., 1993; Hendrix and Meinardi, 2004; Van Maanen et al., 2001; van Loon and Fraters, 2016; De Mars et al., 2024). The

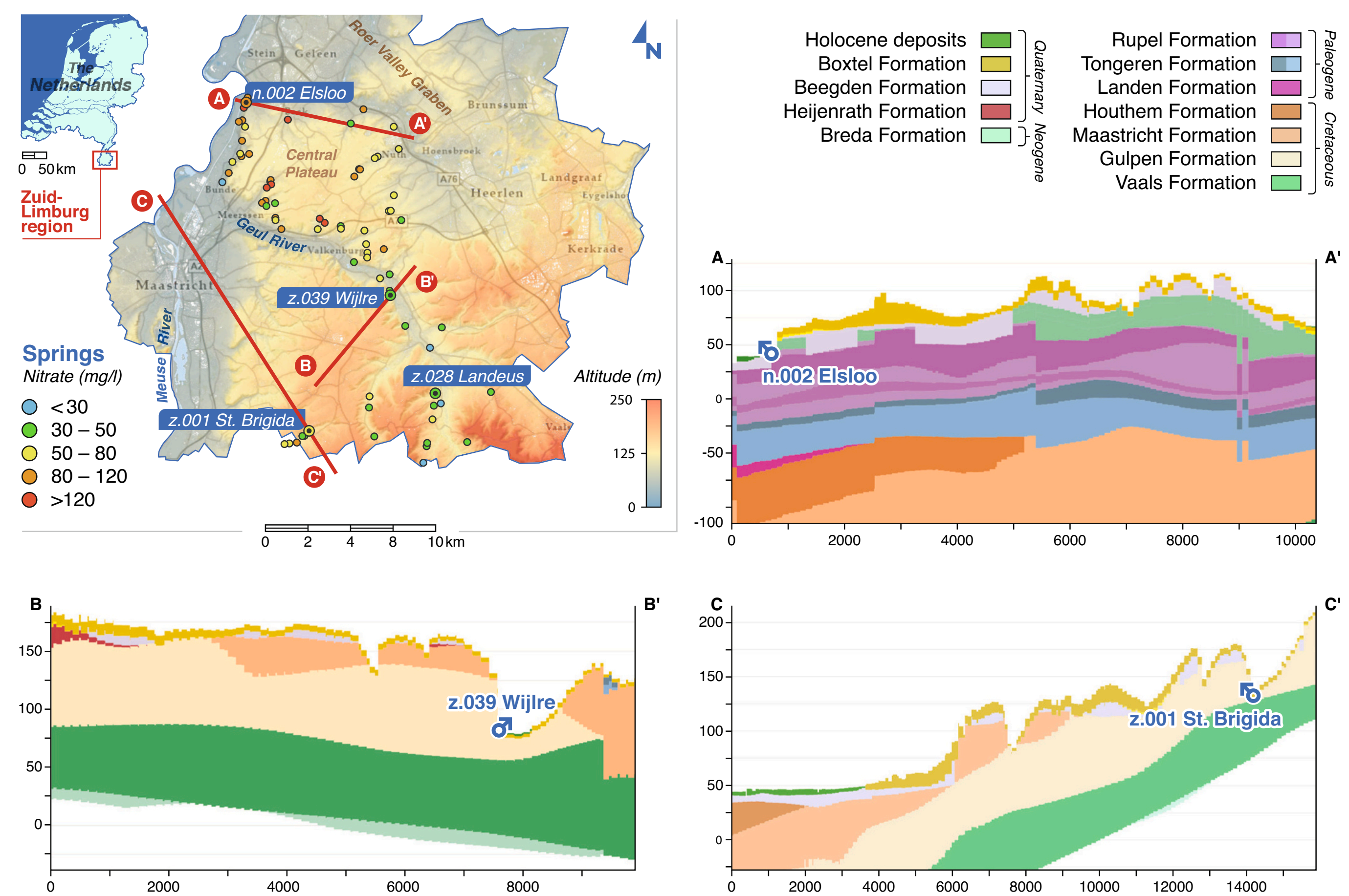

Fig. 1. Elevation map of the study area and the locations of the springs, with their nitrate concentrations in 2009. Hydrogeological cross-sections over 3 selected springs indicate the hydrogeological buildup. The Gulpen and Maastricht formations form the most important chalk aquifers (see main text for details).

climate has mild winters, cool summers, with average temperatures around 11 °C, annual precipitation of 800 mm, and annual evaporation of 600 mm (KNMI, 2020).

2.1.2. Geology

Zuid-Limburg lies on the northern flank of the Rhenish Slate mountains, a chain of low mountains across Germany, Belgium and Luxembourg and the southern Netherlands, composed mainly of Palaeozoic rocks. To the north, it is bounded by the Roer Valley Graben, an active rift zone spanning the southern Netherlands, northeastern Belgium, and North Rhine-Westphalia in Germany (Broers et al., 2021). The Palaeozoic basement dips northwest and is overlain by marine Upper-Cretaceous rocks, and further north, by marine Paleogene and Neogene deposits (Fig. 1). The lowermost Upper-Cretaceous deposits include partly consolidated sands, silts, and clays (Aken and Vaals Formations). The upper part consists of soft limestone (Gulpen, Maastricht and Houthem Formations), similar to chalk deposits in the UK and France (Van Rooijen, 1993; Vernes et al., 2018). The Gulpen Formation contains 50–90 % CaCO3 and glauconite in the lower part, and 80–95 % CaCO3 with flint nodules in the upper part (TNO-GSN, 2020a, 2020b). The Maastricht Formation features soft, fine- to coarse-grained yellow chalky limestones with glauconitic intercalations in the southwest, and alternating hard and soft light gray limestones in the southeast. Younger Paleogene and Neogene deposits are fine to medium sands and clays (Landen, Tongeren, Rupel, and Breda Formations), covered by Quaternary coarse sands and gravels from the former Meuse River (Beegden Formation) and thick loess (Boxtel Formation) on plateaus and hillslopes.

2.1.3. Hydrogeology

The chalk aquifer, comprising the soft limestones of the Gulpen, Maastricht, and Houthem formations, is the main aquifer in Zuid-Limburg and feeds many of the springs (Fig. 1). A subdivision can be made in the area north of the Geul river, where the aquifer is overlain by Paleogene and Neogene deposits (cross-sections A-A' in Fig. 1), and in the area in the south where these deposits are absent (cross-sections B-B' and C-C′). The springs in the southern region drain the chalk aquifer itself, whereas the northern springs mainly drain the shallower Quaternary, Neogene and Paleogene aquifers above the chalk (see Table S1).

The chalk aquifer of the Gulpen and Maastricht formations in the southern region has a saturated thickness of 70 m on average, but locally reaches thicknesses over 150 m (e.g., Fig. 1: cross section B-B′). The thickness of the unsaturated zone of the aquifer varies from around 20–50 m at the centers of the plateaus to 0 m in the valleys of the rivers and brooks where the aquifer is fully saturated. According to Van Rooijen (1993) a mature karst system is not present in the chalk aquifer, although typical karst features are present in the landscape. For example, the southern plateaus exhibit clear sink holes or dolines in the terrain, and narrow and vertical solution pipes, and at the top of the chalk there is evidence for calcite dissolution; residuals of flint-bearing clay and sandy loam are found at the top of the chalk in the southeastern part of the region. Furthermore, dry valleys with a SW-NE orientation are widespread in areas where the chalk aquifer is close to the surface of the plateaus. As in the more famous UK chalks, more pronounced karst features such as caves and subsurface rivers do not occur in our study area, and groundwater flow is presumably a combination of diffuse matrix flow and conduit-controlled flow, with conduits with apertures ranging from millimeters up to a few centimeters (e.g., Worthington and Ford, 2009; Van Rooijen, 1993). Water works in the area indeed show evidence for conduit flow, based on borehole imaging and flow measurements. However, relative to other karst springs in Europe, including ones from the UK chalk, the recession behaviour of the main chalk spring in our study shows a smoothed discharge time series and slow reactions to precipitation events, which are indicative for poorly developed karst (Maréchal et al., 2021; Bailly-Comte et al., 2023). The springs that drain the chalk aquifer are typically located halfway up the dry valleys (St. Brigida spring, z.001, cross-section C-C′), or close to the main river valleys (Wijlre spring, z.039, cross-section B-B′ in Fig. 1), and are often related to contacts between the chalk and less permeable geological formations below, such as the Vaals and Aken formations. Van Lanen et al. (1993) and Teuling (2001) argue that permeable parts of fractured sand- and siltstones in those underlying formations contribute to groundwater flow feeding the springs in the southern region. A few of the chalk springs, including z.028 (Landeus, see Fig. 1) were used for centralized drinking water production but were closed due to increasing nitrate trends.

In the northern part of the region, known as the Central Plateau, the chalk aquifer is covered by a second stratified aquifer of Neogene, Paleogene, and Quaternary deposits with distinct clay layers that act as local aquitards. Hendrix (1985, 1990) showed that the springs in this area generally occur on the slopes of the valleys, at the contacts between permeable layers and aquitards within those Paleogene, Neogene, and Quaternary deposits. Typically, springs at lower elevations drain deeper permeable layers of the Tongeren, Rupel and Breda formations, whereas springs with higher elevations drain the fluvial Beegden Formation (cross section A-A' in Fig. 1). The spring at Elsloo (n.002) mainly drains the Beegden and Breda formations and the permeable upper part of the Rupel Formation.

2.2. Sampling and measurements

A first inventory of nitrate, sulfate and tritium concentrations in 90 springs was conducted in 2001 (Hendrix and Meinardi, 2004) as a follow-up to a more limited nitrate survey in 1984 by Hendrix (1985). The 90 springs were subsequently sampled at eight-year intervals (2009, 2018), generating a time series of tritium, nitrate and sulfate to improve the understanding of the nitrate evolution and forecast future developments based on age distributions (Table S1). For 19 of the 90 springs complementary data were available because they are part of the monitoring network of the province of Limburg, which runs a higher frequency sampling scheme with quarterly nitrate and sulfate data since 2007 (see locations in Fig. S1). Detailed information about field and laboratory methods is provided in Section S1. Tritium concentrations from the 2001 sampling campaign were measured at the Centre for Isotope Research (CIO) of the University of Groningen using gas proportional counting. Tritium samples from 2008 to 2018 were measured at the Bremen Mass Spectrometric facility using the Helium-3 ingrowth method, which involves measuring the accumulated decay product ^{3}He in degassed samples using mass spectrometry after at least 3-months of storage in He-free glass bulbs (Sültenfuß et al., 2009). For 13 springs which are part of the provincial monitoring network of the province of Limburg, additional tritium measurements were performed at three-monthly intervals in 2017 and 2018 to test the range of seasonal variations. Details about the sampling and laboratory methods and the tritium results are provided in Section S1 and Table S2.

2.3. Tritium and nitrate input signals

2.3.1. Tritium in precipitation

A time series of tritium concentrations in precipitation was based on monthly measurements from the closest measurement stations Groningen (1970–1977), Emmerich (1978–2017), and Koblenz (1975–2018) (IAEA/WMO, 2018). The distances from the center of the study area to the Emmerich and Koblenz stations are 110 and 135 km, respectively. The Koblenz station represents a stronger continental effect on tritium concentrations in precipitation than Emmerich; a linear regression between the concentrations at the two stations points to 1.3 times higher tritium concentrations in precipitation in Koblenz and a strong correlation between the two stations (R^2 = 0.97). We assumed an intermediate position between the Koblenz and Emmerich stations for our base case age distribution model and used the two individual stations series for evaluation of model sensitivity (see Section 2.6). For the period before 1970, which lacks regional data, we used data from the Global Network of Isotopes in Precipitation (GNIP; IAEA/WMO, 2018) from Vienna and Ottawa, roughly following Meinardi (1994). The resulting tritium input series is shown in Fig. 2A.

2.3.2. History of nitrate leaching from farmlands

A time series of nitrate concentrations leaching to groundwater was based on results from the monitoring programs that were designed to measure the effects of national and EU legislation (Fig. 2B). Dutch manure policy was implemented since 1984, restricting the use of nutrients in agriculture and restricting the volume of animal manure produced (Henkens and van Keulen, 2001). The EU Nitrates Directive (EU Commission, 1991), aiming to reduce water pollution caused by nitrates from agricultural sources, further tightened regulations, implemented through associated national Nitrate Action Programs. These programs include a system of soil and crop specific application standards for N and P, limits on manure production, and additional measures such as the stimulation of manure exports and the processing of manure, which collectively reduced the nitrogen surplus (see further details in Van Grinsven et al., 2016).

The reconstructed history of nitrate inputs in Zuid-Limburg (Fig. 2B) was based on monitoring data from the National Minerals Policy Network (in Dutch: LMM), which aims to assess the effectiveness of Dutch agricultural mineral policies (Fraters et al., 1998, 2021), and data from the provincial Soil Moisture Network Limburg (SMN; Mak et al., 1999; Ros, 2014), which supports agricultural policies at the regional scale of Zuid-Limburg. Because water levels in the specific Zuid-Limburg region are too deep for sampling the uppermost groundwater, soil moisture is sampled instead from depths between 1.3 and 3.0 m below the surface level (Fraters et al., 2017, 2023). Monitoring data over the period 1996–2021 indicate average concentrations of nitrate leaching to groundwater between 50 and 110 mg/l for arable lands and 50 and 160 mg/l for grassland and silage maize, with an initial decrease over time and stabilization of concentrations since around 2008 (CBS STATLINE, 2023; see Supplementary Info, Section S2 and Table S3 for details). For reconstructing the input history before 1996, we used the nitrogen (N) surplus derived from historical bookkeeping records of minerals applied to farmlands, corrected for crop uptake (Broers and Van der Grift, 2004; Van den Brink et al., 2008; Visser et al., 2007). We performed a linear regression for the period of overlap (1997–2005) between this bookkeeping data series and the soil moisture data, yielding a regression R^2 of 0.98. Based on the regression slope we corrected the bookkeeping data with a factor of 0.73, representing approximately 1.3 times lower N inputs for the Zuid-Limburg plateaus relative to the sandy regions of the adjacent province of Noord-Brabant. Given the strong effect of the introduction of national manure policies since 1984, the peak of N-inputs likely occurred throughout the country at the same time (e.g., Kaandorp et al., 2021). Based on the combination of bookkeeping and soil moisture monitoring data, the resulting N-input series is given in Fig. 2B, showing how nitrate concentrations decreased from around 180 mg/l around 1990 to approximately 60–70 mg/l since 2010. The fluctuations since 1996 represent the actual measured soil moisture data as the best estimate of the nitrogen leaching under the loess plateaus of Zuid-Limburg. Based on the stabilization of measured nitrate inputs and manure production figures, we assumed a constant input of 50 mg/l of nitrate from 2027 onward.

2.4. Assessing age distributions using the shape-free model

To assess age distributions, we applied the shape-free groundwater age model, or age histogram method, previously applied to mixed water in Holten (Visser et al., 2013; Massoudieh et al., 2014) and Noord-Brabant (Broers et al., 2021). An advantage of a shape-free model concept is that it can handle different types of mixing regimes, including mixing waters from two or more separated aquifers and/or dual permeability aquifers, which may, in some cases, lead to bimodal age distributions (Visser et al., 2013; McCallum et al., 2017). Because water in a dual permeability aquifer may include a mix of waters transported

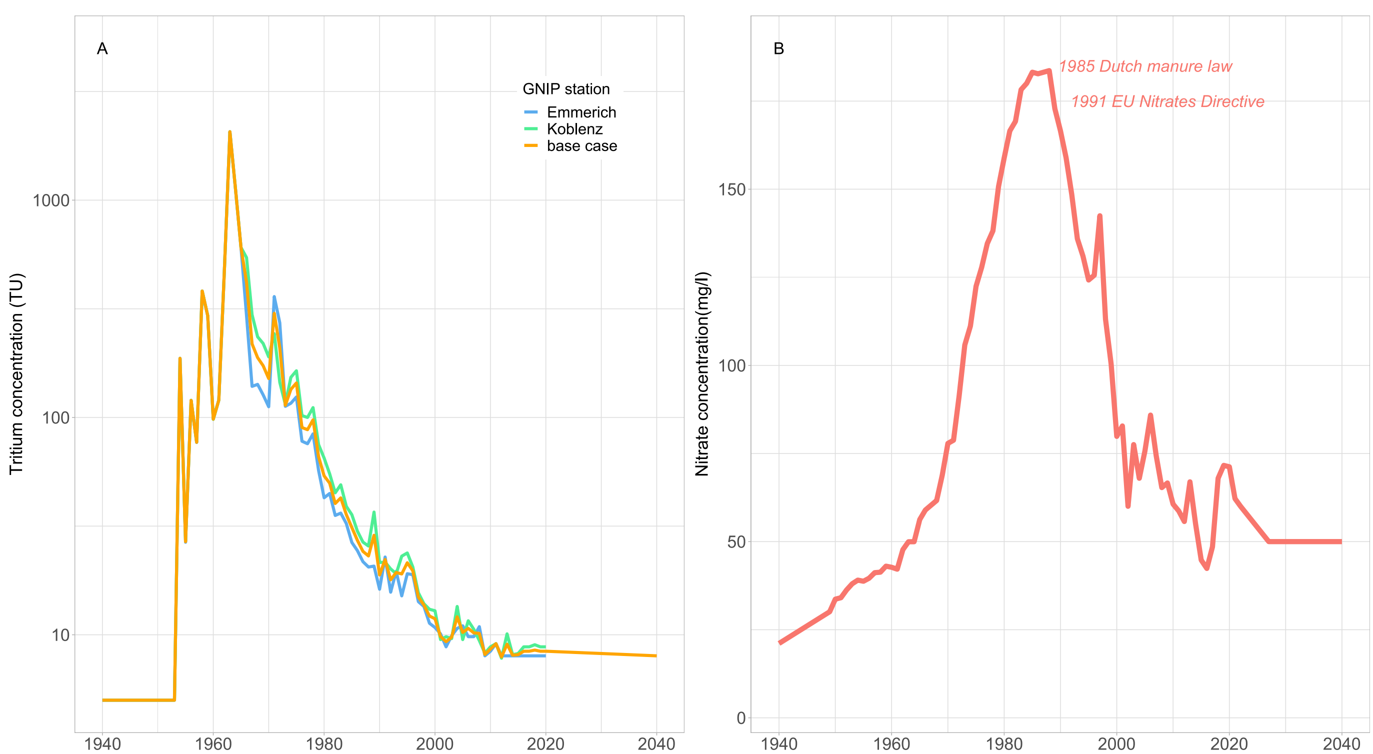

Fig. 2. Time series of tritium concentrations in the GNIP stations Emmerich and Koblenz and time series of the base case variant of the DTTDM model (A; note that the Y-axis is on log-scale.) and reconstructed history of nitrogen inputs to groundwater for the period 1925–2050 (B). The graph shows a clear trend reversal around the year 1985 which can be linked to Dutch and EU legislation to reduce nitrogen leaching from agricultural fields.

by conduit flow and diffuse matrix flow, we did not consider more generic lumped models that make assumptions about the a priori distributions, such as the Exponential model (Vogel, 1967; Maloszewski and Zuber, 1993, 1998), the Dispersion model which assumes mixing along flow paths (Maloszewski and Zuber, 1982; Suckow, 2012; Jurgens et al., 2012, 2016), or the Piston flow model (Eberts et al., 2012; Suckow, 2014). We hypothesize that an age histogram approach such as our Discrete Travel Time Distribution Model (DTTDM) can effectively constrain the age distributions of waters that are mixed at the outflow points of the springs, allowing for a comparison between different springs discharging water from differing hydrogeological and transport settings.

In choosing a shape-free age distribution model, we opted to limit the number of age classes (7) to the limited number of tritium measurements (3 or 4 over the period 2001 tot 2018) and the number of nitrate concentrations (at least 3 to around 25 annual data points over the period 1991 to 2018) to overcome problems of over-parameterization (e.g., Visser et al., 2013; Leray et al., 2016; McCallum et al., 2017). We defined the following 7 age classes to be evaluated using the DTTDM: < 5 years, 5–10 years, 10–15 years, 15–30 years, 30–50 years, 50–80 years, and > 80 years. These age classes reflect the expected range of ages based on the observed tritium concentrations in the springs, which vary between 8 and 25 TU in 2001 and 2.1 and 6.7 TU in 2018, and allow for multimodal distributions while also enabling a young-fraction dominated, near-exponential or piston-flow type shape of the younger part of the age distribution. Moreover, the age classes sufficiently cover the known input history of tritium and nitrate (see Fig. 2) to utilize the differences between tritium-free pre-1950 water, the bomb peak, and the post-1970 decline while convoluting the input series over each TTD. The DTTDM thus consists of a discrete number of 7 bins that were filled with combinations of the 7 age classes using 10 % increments. This leads to a total of 8008 unique mixes, representing all possible TTDs (Visser et al., 2013). The distributions (100 %, 0 %, 0 %, 0 %, 0 %, 0 %, 0 %) and (0 %, 0 %, 0 %, 0 %, 0 %, 0 %, 100 %) form the youngest and oldest possible age distributions, respectively.

Next, we convoluted the nitrate and tritium input series with those 8008 possible distributions, yielding average tritium and nitrate concentrations for each of the 8008 distributions for all monitoring years between 1984 and 2018 by linearly mixing the concentrations in each of the 7 bins, weighing the proportion of the age classes in each of the bins. For example: one of the 8008 distributions might have 10 % water younger than 5 years (1st bin), 10 % between 5 and 10 years (2nd bin), 20 % between 10 and 15 years (3rd bin), 20 % between 15 and 30 years (4th bin), 20 % between 30 and 50 years (5th bin), 20 % between 50 and 80 years (6th bin), and 0 % > 80 years (7th bin). For this hypothetical age distribution, we find the following computed tracer concentrations in the year 2009: 11.8 TU tritium and 94.4 mg/l nitrate.

Subsequently, we compared the computed series of tritium and nitrate outcomes of the 8008 possible distributions with the measured tritium and nitrate series at the springs, optimizing for the best fit between measurements and models. The best-fit models were identified based on the deviations between modelled and measured time series using a least-squares approach, which weighs the measurement uncertainty of the measured tritium and nitrate concentrations for the years in which measurements were available:

$$\chi^2_{tritium} = \frac{\sum_{\mathrm{year}=1}^{n} \left(\frac{\left(\mathrm{tritium_{DTTDM}} - \mathrm{tritium_{spring}}\right)^2_{\mathrm{year}}}{\left(\mathrm{tritium_{uncertainty}}\right)^2} \right)}{\mathrm{n}} \tag{1}$$

$$\chi^2_{\mathrm{nitrate}} = \frac{\sum_{\mathrm{year}=1}^{n} \left(\frac{\left(\mathrm{nitrate_{DTTDM}} - \mathrm{nitrate_{spring}}\right)^2_{\mathrm{year}}}{\left(\mathrm{nitrate_{uncertainty}}\right)^2} \right)}{\mathrm{n}} \tag{2}$$

where n is the number of years for which ^{3}H or nitrate measurements are available. Weighing the number of measurement years results in equal weights for nitrate and tritium information when summing the two results in the base case scenario. We chose the average of the 50 best-fit models (lowest χ^2_{sum} to determine the average age distribution and used the 50 best-fit TTD models to calculate a standard deviation for the proportions of the 7 age classes for each of the individual springs.

2.5. Age distribution metrics

In discussing the results, we used the following summarizing metrics of the age distribution: Mean Travel Time (MTT), fraction of young water and fraction of old water. Here, we define young water as water with an age smaller than 30 years, and old water as water with an age over 80 years. The fraction of young water thus includes the fractions of the first four age bins. The MTT was calculated by summing products of the mean ages in the seven age bins of the TTD and the corresponding fractions f_i, assuming a uniform age distribution in each bin:

$$\mathrm{MTT} = \sum_{i=1}^{7} \overline{age_i} \times f_i \tag{3}$$

For the example distribution discussed in Section 2.4 this yields an MTT of 29 years.

2.6. Reconstructing and forecasting nitrate evolution

For each specific spring, the 50 best-fit TTD models were convoluted with the tritium and nitrate input series to obtain a modelled time series of tritium and nitrate concentrations, which includes a forecast for the average concentration and an indication of the uncertainty based on the 50 best-fit TTD models.

We tested the robustness of the DTTDM approach using a simple sensitivity analysis, comparing the results of the base case model runs with a number of alternative setups (Table 1). The aim of the sensitivity analysis was to test whether the DTTDM approach is robust and whether uncertainties are sufficiently small to evaluate the past and future spring nitrate time series on the basis of their age distributions. Alternative model runs 1 and 2 assessed the uncertainties involved in applying either the Emmerich or the Koblenz tritium time series in precipitation (see section S3 in the Supplementary Information). Alternative model runs 3 to 6 tested the effects of different weight factors (3,10) for the nitrate and tritium least-squares evaluation. In model runs 7 and 8, we tested the effects of respectively 15 % increased or decreased nitrate leaching relative to the base case model nitrate input of Fig. 2B. In model run 9, we tested whether high temporal sampling of nitrate, as done in the springs which are part of the monitoring network of Limburg (Fig. S1), would change the general outcomes. Finally, in model runs 10 and 11 we tested whether the assumption of conservative transport is valid for the springs which have a supposed contribution of flow through the Vaals Formation, assuming nitrate reduction in the older water fraction (Table 1 and section S5).

3. Results and discussion

3.1. Nitrate, tritium and the fraction of young water

Fig. 3 shows the resulting fits of the nitrate and tritium concentration data for three of the springs marked in Fig. 1. Here, red dots indicate measurements done for the National Monitoring Network, and purple dots represent measurements from the provincial monitoring network of Limburg. The three springs showed noticeable differences in their measured tritium concentrations over time and their nitrate response, as well as their modelled fit. Spring n.002 (Elsloo) presents relatively high initial nitrate and tritium concentrations in 2001 and a relatively rapid decline in nitrate and tritium concentrations between 2001 and 2018 (Fig. 3A). The age histogram derived from the 50 best-fit DTTDM models indicates that almost all of the discharging groundwater has infiltrated

Table 1
Summary of the sensitivity analysis runs for the base case model and alternative setups.

Nr	Run	Tritium input	Nitrate input	Tritium weight	Nitrate weight	Sampling frequency	Denitrification
0	Base case	Emm/Kobl	Fig. 2B	1	1	no	none
1	Emmerich series	Emmerich	Fig. 2B	1	1	no	none
2	Koblenz series	Koblenz	Fig. 2B	1	1	no	none
3	Tritium weight 3 x	Emm/Kobl	Fig. 2B	3	1	no	none
4	Tritium weight 10 x	Emm/Kobl	Fig. 2B	10	1	no	none
5	Nitrate weight 3 x	Emm/Kobl	Fig. 2B	1	3	no	none
6	Nitrate weight 10 x	Emm/Kobl	Fig. 2B	1	10	no	none
7	Higher nitrate input	Emm/Kobl	Fig. 2B * 1.15	1	1	no	none
8	Lower nitrate input	Emm/Kobl	Fig. 2B / 1.15	1	1	no	none
9	Sampling frequency	Emm/Kobl	Fig. 2B	1	1	yes	none
10	Some denitrification	Emm/Kobl	Fig. 2B	1	1	no	90 % reduction after 50 years
11	Stringent denitrification	Emm/Kobl	Fig. 2B	1	1	no	Run 10 + 50 % reduction after 30 years

Emm/Kobl = combined GNIP series of Emmerich and Koblenz stations (see text).

less than 30 years ago. Following our definition of the fraction of young water including all water < 30 years old, this fraction is 0.96 for spring n.002. Spring z.039 (Wijlre) is on the other side of the age spectrum with a young fraction of 0.22 (Fig. 3C). Its tritium time series shows lower tritium levels in 2001 and a more gradual decrease over time. Please note that seasonal variations in tritium are very limited for all these springs, for which quarterly measurements were available over 2017 and part of 2018 (see Supplementary Information, Table S2). The nitrate concentrations in spring z.039 range between 30 and 45 mg/l and do not show a convincing downward trend or a nitrate peak in a specific year. Spring z.001 (St. Brigida) takes an intermediate position between the two forementioned springs (Fig. 3B): its tritium decline is substantial; it shows a clear nitrate peak around the year 2000, but its nitrate concentrations are substantially lower and the decline more gradual relative to spring n.002. The average histogram of the DTTDM model suggests a multimodal age distribution with a moderate fraction of young water (0.50) and a substantial old fraction (defined as >80 years old, 0.33).

As highlighted in Fig. 1, the springs drain different parts of the subsurface of Zuid-Limburg. Spring n.002 (Elsloo) drains Paleogene, Neogene and Quaternary sands and gravels at the Central Plateau, whereas springs z.039 (Wijlre) and z.001 (St. Brigida) drain the chalk aquifer of the Gulpen Formation. Spring z.039 presents an outlet in one of the main brook valleys, whereas spring z.001 discharges at a substantially more elevated position, halfway up a dry valley with SW-NE orientation. For spring z.001 the flow contribution from the chalk is presumably complemented by a contribution from the underlying fractured sandstones of the Vaals Formation (see also Section 3.3). Fig. 4 confirms the difference between the springs draining the Paleogene, Neogene and Quaternary formations in the north and the chalk springs in the south; large fractions of young water are dominant in the north, whereas moderate and low fractions dominate the south of the study area.

Fig. 4A demonstrates that the fraction of young water is correlated with the concentration of nitrate, whereas the Mean Travel Time (MTT) is inversely correlated with nitrate (Fig. 4B). Moreover, the decline in nitrate concentrations between 2001 and 2008 is more pronounced in the springs with high fractions of young water (arrows in Fig. 4A). Most of these springs with initially high but rapidly declining nitrate concentrations are centered around the northerly Central Plateau, at the outcrops of permeable sands and gravels from the Paleogene, Neogene, and Quaternary formations. The low to moderate thickness and associated volume of those aquifers and low volume over (precipitation) flux ratios are suggested to be the main drivers of the short MTTs (e.g., Vogel, 1967; Van Ommen, 1986). In such thin aquifers, this results in a groundwater system that becomes fully saturated with nitrate, leading to high nitrate concentrations in the outflow and a quicker response to decreasing inputs.

On the contrary, springs in the main river valleys show relatively small fractions of young water, moderate to low nitrate, and a more gradual decrease in concentrations. The models point towards multimodal or bimodal age distributions for the springs that drain the chalk plateaus, suggesting the mixing of young and old water components near the system outlets. Specifically, spring z.039 (Wijlre) drains a relatively thick sequence of chalk, which explains its relatively high volume-to-flux ratio and the associated long Mean Transit Times (MTTs) (see Fig. 1, cross-section B-B′). This implies that these aquifers contain a depth-stratified nitrate profile, with nitrate-free waters in the deeper parts. Consequently, this leads to the dilution of nitrate concentrations at the spring outflow. Spring z.001 (St. Brigida) drains the chalk aquifer halfway up a dry valley and has an intermediate position with a clear trend reversal in nitrate, but at lower concentrations than the northerly springs. These differences in nitrate concentrations cannot easily be explained by land use differences between the northern and southern plateaus (see Supplementary Information, section S2). Nitrate concentrations in springs on the northern plateau decrease faster than nitrate concentrations on the southerly plateaus, showing how measures to reduce N applications in farming affect nitrate concentrations in different springs differently, depending on the age distribution of the outflowing water. Overall, the results reveal that the concentration levels of nitrate and the trend evolution are strongly correlated with both the fraction of water aged <30 years and the mean travel time. This conclusion is largely in line with Solder et al. (2016), who argue that groundwater flow systems with a larger proportion of old water are less variable and less sensitive to hydrologic variability than groundwater flow systems with a smaller proportion of old water, because the magnitude and timing of groundwater discharge, driven by variation in climate and water use, is expected to be dampened and attenuated for systems with larger dynamic storage volumes and longer MTTs.

Both the fraction of young water (<30 years) and the MTT are fairly insensitive to the use of alternative tritium input series, the weight factors for the nitrate and tritium least-squares evaluation, and the level of nitrate leaching (see Supplementary Information, section S3 for details on the sensitivity analysis). For example, the sensitivity analysis revealed that varying the input curves of nitrate and tritium or the aforementioned weight factors do not fundamentally alter the ordering of springs by the fraction of young water or the MTT, nor impose large deviations between the fractions or MTT of the base case model and the alternative models for the large majority of the springs. Only increasing the weight of tritium over nitrate in the least-squares evaluation 10-fold yielded a meaningful perturbation with a compressing effect on the range of MTTs: short MTTs tended to increase while long MTTs generally decreased. From the sensitivity assessment, we concluded that the DTTDM approach is robust for determining the young fractions and the MTT when both tritium and nitrate time series are included, which is in line with earlier conclusions from Alikhani et al. (2016) for a number of nitrate-contaminated public supply wells in California. Therefore, we determined that the differences between the alternatives and the base model are sufficiently small to assess and order the springs based on

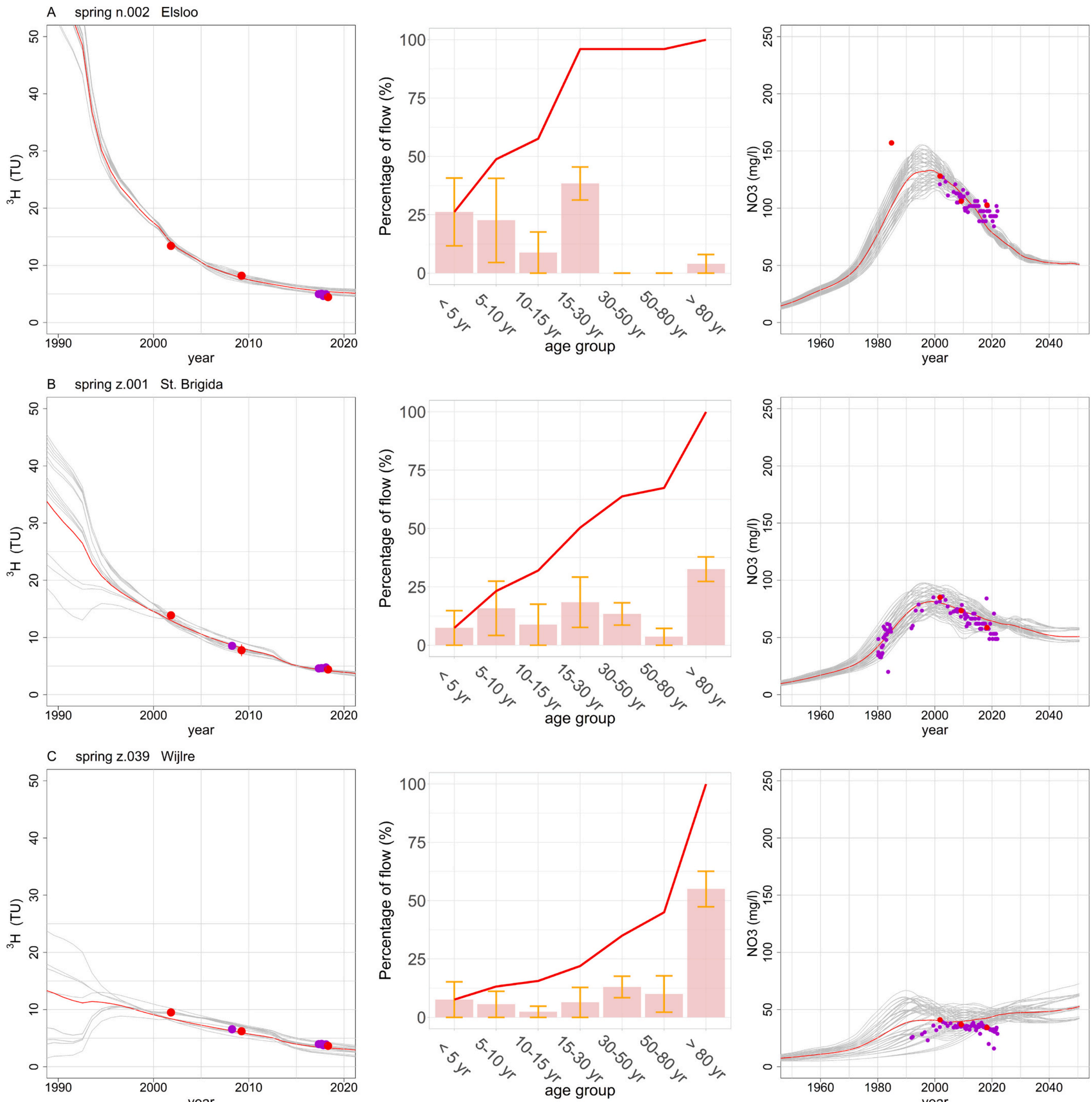

Fig. 3. Age histogram (pink boxes), cumulative age distribution (red line, center panel), and fits of the tritium (left panels) and nitrate (right panels) time series for 3 springs: A. n.002 (Elsloo), B. z.001 (St. Brigida), and C. z.039 (Wijlre) for the base model. The red line indicates the average of the 50 best fits, and gray lines indicate the individual 50 best fits. Red dots indicate measurements done for the National Monitoring Network (LMM). Purple dots represent measurements from the provincial monitoring network of Limburg. See Fig. 1 for the location of the springs.

their young fractions and MTT and use the results for evaluating the nitrate trend reversal and the long-term tail of the nitrate evolution.

3.2. Nitrate trend reversal in relation to MTT

We further evaluated how the age distributions affect the timing and height of the nitrate peak and the probable future evolution of nitrate concentrations, assuming a stabilization of leached nitrate in line with current agricultural practices and trends (see Supplementary Information, section S2). Therefore, we classified the springs into classes with comparable MTT (Fig. 5) and evaluated the measured concentrations between 1984, 2001, 2009, and 2018 (boxplots), and the modelled nitrate concentrations over the period 1925 to 2050, using the results of the base case model. A clear trend reversal of measured nitrate concentrations is indicated by the boxplots in Fig. 5A-D, with generally lower concentrations in 1984, peak concentrations in 2001, and a decline afterwards. The model fits generally follow this measured trend reversal, as reflected in the shape of the gray lines in Fig. 5. The Figure also shows that the nitrate response after the 1985 peak in nitrogen application differs clearly between springs with short and long

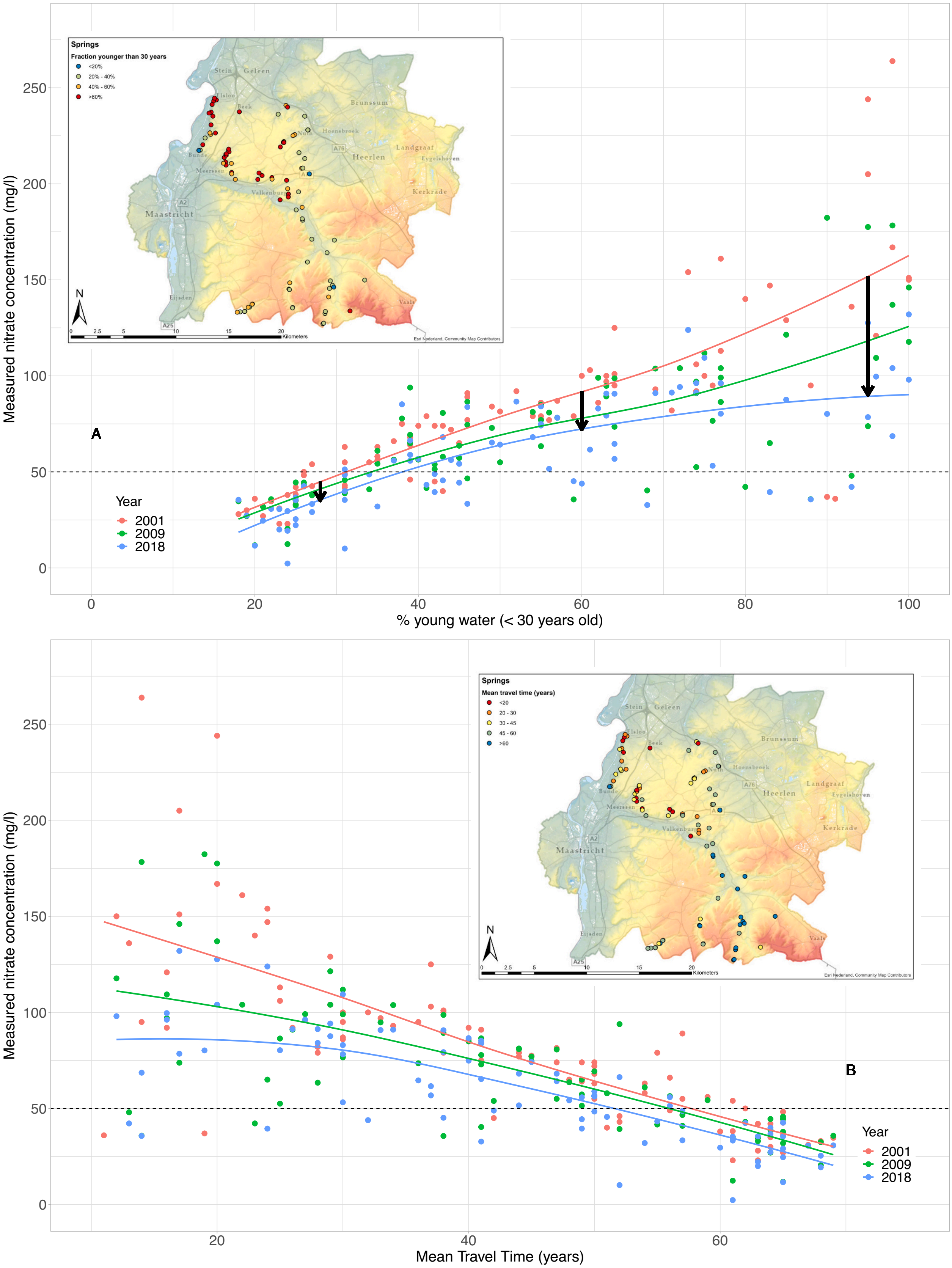

Fig. 4. Relations between the evolution of nitrate concentrations over the years 2001 to 2018 and the fraction of young water (A) and the Mean Travel Time (B). Arrows denote the concentration decline between 2001 and 2018. High initial nitrate concentrations and fast declines are associated with a large fraction of young water and short MTT. The maps show the spatial patterns of the young fraction and MTT, with shorter MTT at the northern plateaus. Colored lines represent the LOWESS smooths for 2001, 2009, and 2018, summarizing the local median of the data scatter (Cleveland and Devlin, 1988).

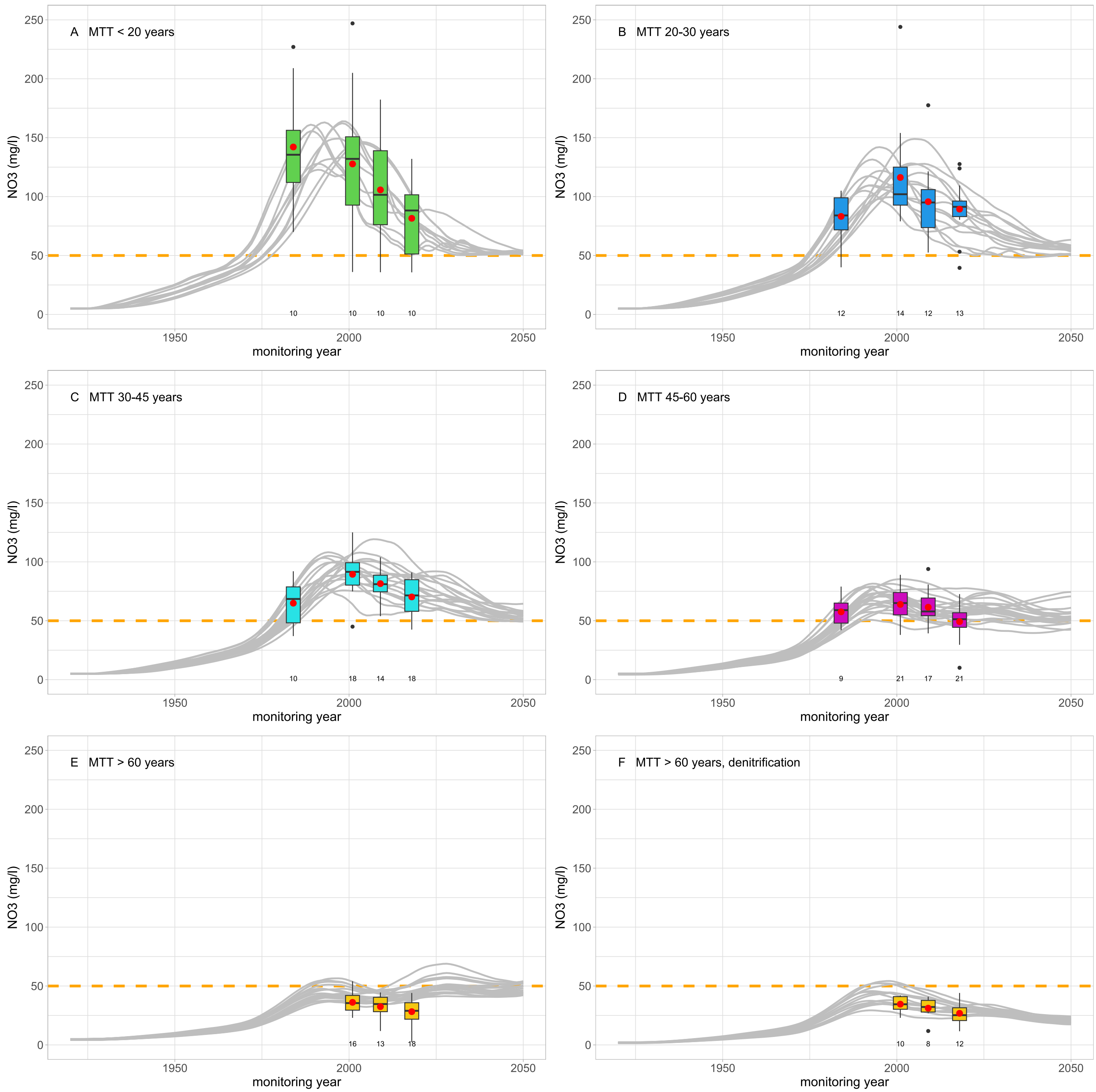

Fig. 5. Trend reversal of nitrate in spring water as a function of Mean Travel Time for the conservative base case model (panels A-E). Boxplots summarize the measured concentration distribution for springs that fall within the specified MTT class (numbers indicate the number of samples for each boxplot), and gray lines represent the best-fit models for each of the springs within that MTT class. The 50 mg/l threshold of the EU Nitrates and Groundwater Directives is shown for reference (orange). Panel F shows the result of alternative model run 11, in which stringent denitrification was assumed, which might explain the observed concentration decline in springs with high MTT (see Section 3.3 of the main text).

MTTs (Fig. 5 and Table 2).

Table 2 summarizes the findings for the measured average nitrate concentration in 2001, the modelled nitrate peak concentrations, the lag time between the peak in nitrogen applications in 1985 and the peak of nitrate concentrations in the spring, and the steepness of the nitrate decline between 2001 and 2018. In the table, we chose the 2001 measured data as a reference for the modelled peak because 2001 resembles the peak moment for most of the springs. Evidently, measures to reduce N in farming affect the nitrate evolution at different springs differently, depending on the distribution of ages in the discharging spring water. The springs with an MTT below 20 years show high nitrate concentrations in 2001 (141 mg/l), a high modelled nitrate peak (146 mg/l), a steep decline (2.9 mg/l per year), and a short lag time between the leaching peak in 1985 and the peak at the spring (10 years on average, see Table 2). For springs with longer MTTs the peak concentrations and the steepness of the decline decrease, whereas the lag time increases (Table 2, Fig. 5). Both the *age fraction < 30 years* and the *MTT* have large explanatory power for the peak nitrate concentration and the steepness of the decline in nitrate concentrations between 2001 and 2018 (Fig. 6; see also Supporting Information, section S4 and Fig. S5).

Table 2
Average level of the modelled nitrate peak, the time to peak and the speed of nitrate decline from 2001 to 2018, averaged for the five MTT classes distinguished in Fig. 5. The upper part of the table refers to the conservative base case model. The lower part of the table refers to an alternative model setup with denitrification (see Section 3.3 for details).

	Monitoring	DTTDM results (averaged over the MTT age class)		
Age class	Average nitrate 2001 (mg/l)	Average nitrate peak (mg/l)	Lag time to peak (years after 1985)	Nitrate decline 2001–2018 (mg/l yr^{-1})
Base case				
MTT < 20 years	141	148 ± 14	10 ± 5	2.9
20 < MTT < 30 years	116	121 ± 14	14 ± 7	1.6
30 < MTT < 45 years	89	94 ± 14	16 ± 8	0.8
45 < MTT < 60 years	65	72 ± 7	21 ± 18	0.4
MTT > 60 years	37	52 ± 6	46 ± 16	−0.1
Stringent denitrification case				
MTT < 20 years	141	148 ± 14	10 ± 5	3.0
20 < MTT < 30 years	116	121 ± 14	14 ± 6	2.0
30 < MTT < 45 years	89	89 ± 14	16 ± 5	1.2
45 < MTT < 60 years	65	60 ± 13	12 ± 4	0.8
MTT > 60 years	37	42 ± 8	11 ± 3	0.5

However, for the *lag time* between the peak in nitrate leaching in 1985 and the peak of nitrate concentrations in the spring, the largest explanatory power comes from the *age fraction < 15 years* (Fig. 6). We interpret the importance of the very young water fraction (< 15 years) as an effect of unsaturated zone delay (e.g., Ascott et al., 2017). Infiltrating water in areas with deep unsaturated zones will only start contributing to saturated zone flow towards the spring once the water has drained from the unsaturated zone. As many of the springs at the northerly Central Plateau drain the more elevated parts of the aquifer system and vertical flow is limited by the presence of aquitards, their unsaturated zones are shallower, and a larger fraction of water aged <15 years will reach the springs. Conversely, for the springs draining the chalk aquifer with more developed unsaturated zones at the southern plateaus, only a limited fraction of infiltrating water reaches the saturated zone in the first 15 years, which extends the lag times.

These results resemble those of Van der Velde et al. (2010) and Kaandorp et al. (2021), who studied the determining factors for lag times for two brook valleys in the east of the Netherlands. Based on limited time series of tritium measurements and long-term nitrate time series, Kaandorp et al. (2021) argued that groundwater age distribution is a key factor for the lag time between nitrate leaching and spring outflow. They identified several variables that may determine the lag time, including the unsaturated zone delay and the distance between agricultural fields and the outflow points of the groundwater system (see also Wang et al., 2013). Relative to this earlier work, our current benefits from the large number of springs for which long-term tritium and nitrate time series are available, the diverging hydrogeological settings of the springs, and local measurements of root zone nitrate leaching (see Supporting Information, section S2). In our case, the distance from farmlands to the springs is less of a factor, because the loess plateaus are entirely in agricultural use and because differences in nitrogen leaching between the plateaus are limited (Supporting Information, text S2). Our results show that positive nitrate trends can be reversed within a time frame of 10 to 25 years after measures to reduce leaching from the root zone are employed, even in areas with relatively deep unsaturated zones, such as the loess and chalk plateaus in Zuid-Limburg. Since the *fraction of young water* and the *MTT* are quite insensitive to alternative model setups, we assume that the same holds for the peak nitrate concentrations and the slope of nitrate decline afterwards, which are well explained by these age distribution variables. Likely, the same holds for the prolonged tailing of the nitrate concentrations, which is discussed in the next section.

3.3. The prolonged tail of the nitrate evolution: nitrate legacy

Monitoring results of the root zone leachate at the loess plateaus showed that soil moisture nitrate concentrations have stabilized since around 2010 and have little tendency to decrease because large further reductions in manure and fertilizer applications are not foreseen (Van Boekel et al., 2021; see section S2 of the Supporting Information). Therefore, we assumed that nitrate leaching stabilized at a

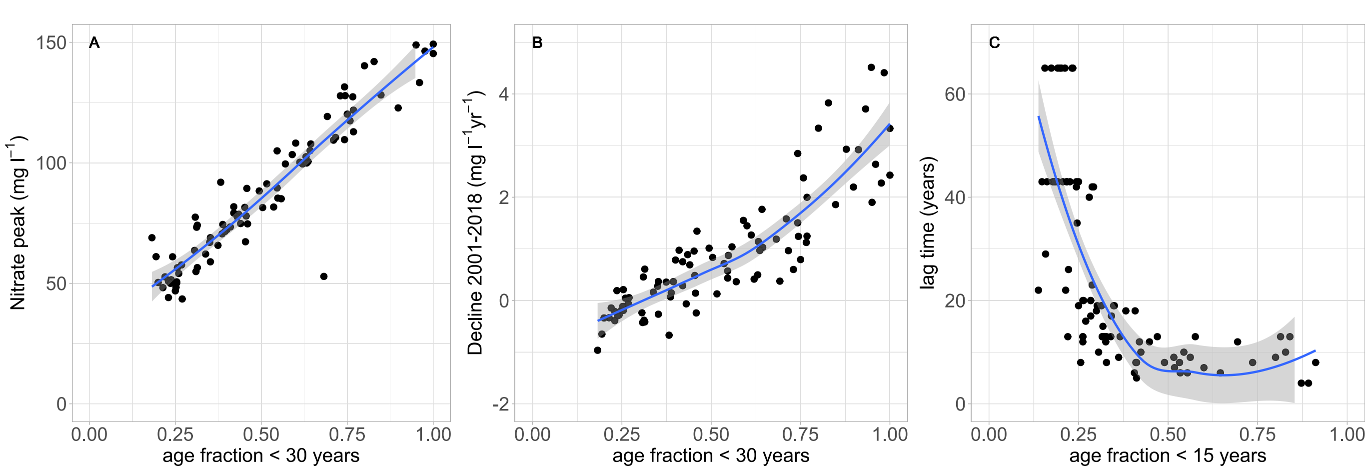

Fig. 6. Explanatory power of the *fraction <30 years* for the modelled nitrate peak (A) and the modelled decline from 2011 to 2018 (B) and for the *fraction <15 years* for the lag time between the leaching peak and the peak concentration at the spring (C). Lines represent the LOWESS smooth, summarizing the local median of the data scatter (Cleveland and Devlin, 1988).

concentration level of 50 mg/l from 2027 onward and used that as a model constraint. As a result of this model assumption, and the assumption of conservative transport, nitrate concentrations in all the springs will eventually equilibrate at this concentration level, although at different moments in time, depending on their age distributions.

We modelled the nitrate concentration as a function of the fraction of young water and the MTT for the years 2001 and 2018, along with the simulated forecasts for 2027 and 2035 (Fig. 7). The year 2027 serves as an evaluation milestone in the EU Water Framework and Groundwater Directives, when water quality should comply with the goals set in 2000. The conservative base case model results suggest that only springs with a small fraction of young water (< 25 %) or a mean travel time > 60 years will meet the EU groundwater quality standard of 50 mg/l in 2027 (Fig. 7A and C). A relatively fast decrease towards the equilibration level of 50 mg/l occurs at the springs with a large fraction of young water, and the slowest decrease towards this level appears around an MTT of approximately 30 to 40 years.

Both the 2027 and 2035 forecasts are fairly insensitive to the use of alternative tritium input series and to the weight factors for the nitrate and tritium least-squares evaluation (see Supplementary Information, section S3 for details). Logically, the forecasts are sensitive to the input concentrations of nitrate leaching, especially affecting springs with large fractions of young water. However, the largest uncertainty in the forecasted concentrations for 2027 and 2035 is related to the possibility that reactive processes may attenuate nitrate concentrations in springs that are partly fed from the Vaals Formation. Indications for such processes arise from increasing sulfate concentrations in several chalk springs in the southern region, combined with a stronger decrease in nitrate concentrations than simulated by the conservative base case model. This is visible in Fig. 5E, where the measured nitrate concentrations are below the modelled concentrations and show a declining trend and an earlier trend reversal which are not supported by the 50-best-fit conservative base case models (for more details, see also Supplementary Information, section S4). Therefore, we tested two alternative models in which denitrification coupled to pyrite oxidation (e.g., Zhang et al., 2009, 2012) could remove nitrate from part of the outflowing groundwater while mobilizing sulfate. The first model assumed a 90 % reduction after 50 years of travel time. The second model was more stringent and assumed a 50 % nitrate reduction after 30 years and 90 % after 50 years of travel time. Only the second model was able to mimic the nitrate decline and earlier trend reversal in the springs with MTTs >60 years, as illustrated in Fig. 5F (see Section S5 and Figs. S6, S7, and S8 for details).

This denitrification model is better suited for replicating the 2001 measured concentrations for springs with longer MTTs (Table 2) and capturing the observed earlier trend reversal and subsequent decline in concentrations between 2001 and 2018 in those springs. Clearly, the application of this denitrification model to the southern chalk springs has substantial implications for the 2027 and 2035 forecasts, particularly impacting springs with smaller young water fractions and higher MTTs (Fig. 7B and D). This adjustment results in a larger proportion of southern springs being forecasted to fall below the 50 mg/l EU groundwater quality standard in 2027. Notably, the integration of reactive processes also diminishes the lag times between the leaching peak and the nitrate peak in the outflowing water. This reduction is primarily dictated by the younger fraction of water, which remains unaffected by the denitrification process (see section S5 of the

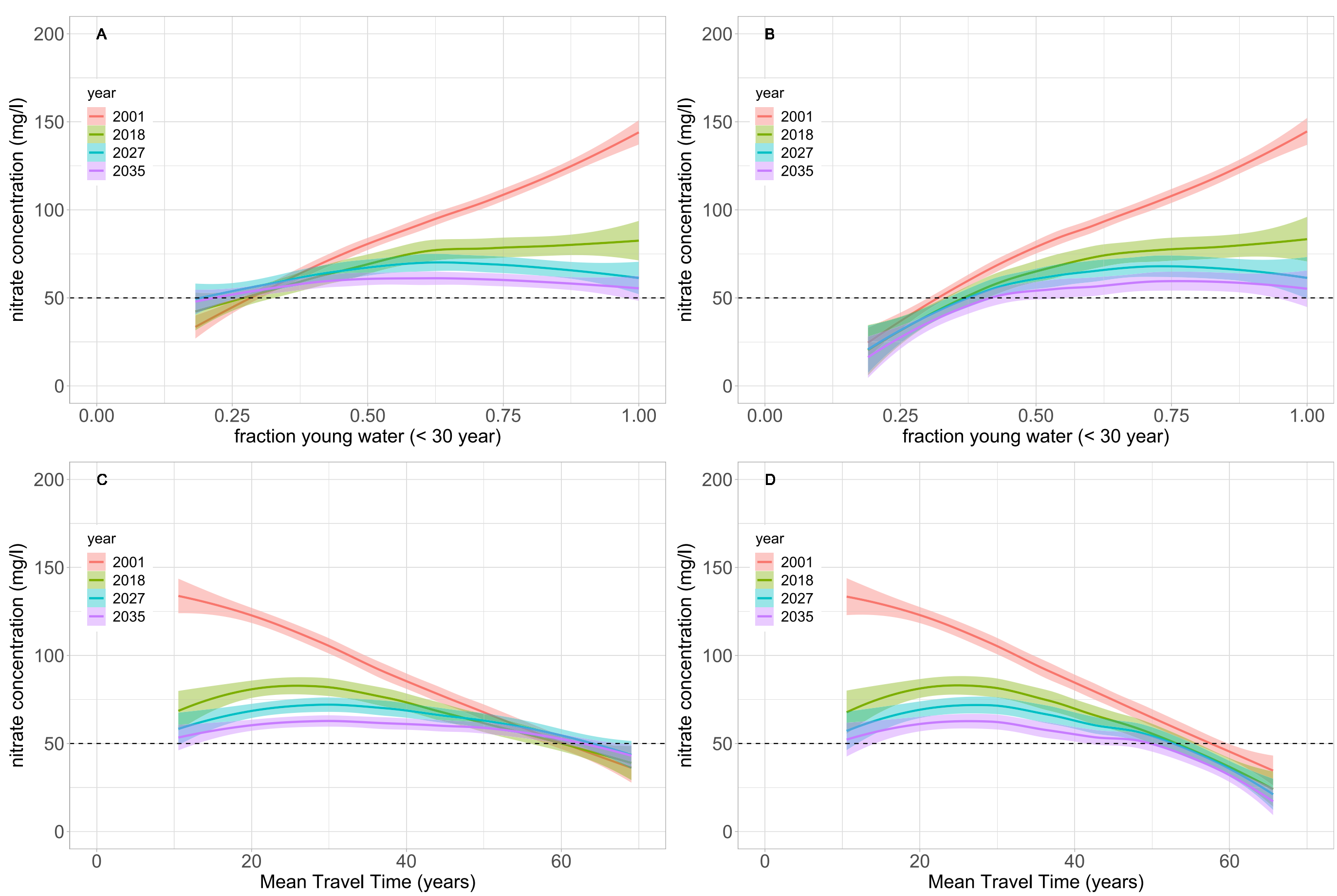

Fig. 7. Modelled nitrate concentrations as a function of the *fraction of young water* (A and B) and *MTT* (C and D) for 2001, 2018, 2027 and 2035 for the base case model assuming conservative transport (A and C) and a model with stringent denitrification in the southern springs (B and D). Lines and dashed areas represent the LOWESS smooth and its uncertainty, summarizing the local median of the data scatter for each of the modelled years (Cleveland and Devlin, 1988).

Supporting Information). Consequently, lag times vary between 10 and 16 years for all the examined springs after incorporating potential denitrification processes in the southern springs (Table 2). This underscores the efficacy of trend reversal achieved by measures aimed at reducing contaminant leaching, even in regions characterized by thick unsaturated zones.

The tailing of nitrate concentrations in springs with longer MTTs aligns with the hypotheses put forward by Ascott et al. (2017), reflecting the slow release of nitrate stored in the vadose and saturated zones. However, as shown in Fig. 7C and D, the tailing towards the stabilization level of 50 mg/l is most prominent around an MTT of approximately 30 to 40 years, whereas springs with longer MTTs exhibited lower nitrate peaks due to substantial dilution by nitrate-free old water components, resulting in a delayed and attenuated response. This delayed and attenuated response is also evident from the strong hysteresis of spring outflow concentrations relative to leachate inputs, as illustrated for selected contrasting springs in Section S6 and Fig. S9 of the Supplementary Information. Overall, the hysteresis plots elucidate the loading of the groundwater system with nitrate, showing an initial slow increase in spring concentrations attributed to the contribution of nitrate-free, pre-1960 water, followed by a delayed reaction after the input load began to decrease post-1985. Assuming conservative transport, the hysteresis patterns are entirely determined by the age distribution of the discharged water at the spring, while subsurface denitrification influences the shape in reactive cases. These conclusions corroborate earlier findings by Sarrazin et al. (2022), whose sensitivity analysis highlighted the travel time and denitrification rate in the subsurface as important determinants of nitrogen legacies in receiving surface waters.

In conclusion, the N legacy is more prominently reflected in the prolonged tail of elevated nitrate concentrations post-2020 than in the lag time of the concentration peak. The study demonstrates that farmers have successfully reduced soil N surpluses, resulting in evident trend reversals at all springs within a time lag of 10–15 years. The persistent tailing after the trend reversal is primarily attributed to the ongoing leaching of nitrogen from agricultural fields and the associated nitrate loading of the groundwater system since 1985 that persists to the present day, which aligns with previous work by Kaandorp et al. (2021). Under conservative transport assumptions, the springs, regardless of their MTTs, ultimately reach equilibrium with input nitrate concentrations influenced by prolonged agricultural practices. However, this alignment occurs at various chronological points corresponding to their age distribution. Areas featuring thick unsaturated zones and/or high-volume aquifers with prolonged MTTs tend to exhibit lower nitrate concentrations than springs with shorter MTTs. This distinction arises from the contribution of nitrate-free old water, originating from the era preceding the agricultural nitrate peak. Despite popular references to a “legacy nitrate time bomb” (Wang et al., 2013), our study reveals that this metaphorical time bomb undergoes significant dilution during outflow, predominantly influencing the enduring tail of nitrate contamination rather than the peak concentrations at the outlets.

3.4. *Implications for nature reserves, ecological objectives and public water supply*

The study underscores the necessity for further reductions in agricultural nitrate leaching to achieve lower nitrate concentrations in the springs. This is particularly relevant for meeting nutrient threshold values, such as the proposed 18 mg NO_3/l for endangered bryophyte-dominated Natura2000 habitats (De Mars et al., 2024), based on a subset of the springs in this study. Additionally, water discharged at the springs feeds the regional brook system, which must meet surface water quality standards and ecological objectives under the EU Water Framework Directive (2000/60/EC). This includes a 2.3 mg N/l standard for total nitrogen (Provincie Limburg, 2021), equivalent to approximately 10 mg NO_3/l. Despite subsurface denitrification reducing concentrations at some spring outlets, meeting these standards and the proposed Natura2000 levels seems unlikely in the foreseeable future.

The enduring influence of nitrate pollution in the region is closely linked to the sustained, continuous groundwater loading. This loading is expected to persist due to a lack of progress in reducing N inputs over the past decade (Kros et al., 2024), with reports of increasing N emissions in some instances (CBS, 2023). Climatic effects have also led to temporarily higher nitrate concentrations in soil moisture following the 2018 drought (see the upward impulse in Fig. 2B in 2019 and 2020). Consequently, a 50 mg/l input concentration was used as a conservative estimate in our forecast models for the period after 2027 (see Section 3.3). Results indicate that nitrate concentrations across all studied springs will eventually stabilize at this average leachate input concentration, though at different times depending on their travel time distribution. Springs with intermediate MTTs (30–40 years) showed slower stabilization than those with short MTTs, leading to higher concentrations in the 2027 and 2035 forecasts (Fig. 7). This holds practical significance from a management perspective, as exemplified by the nitrate concentration trends at spring z.028 (Landeus, Fig. 1 and Fig. S7), a source tapped for public water supply. The facility's closure in 1988 due to rising nitrate concentrations ironically saw concentrations drop below the EU drinking water standard of 50 mg/l around 2000. This trend reversal was due to denitrification in the fractured sandstones of the Vaals Formation, affecting peak concentrations and lag time between leachate and outflow peaks (see Section 3.3). This example highlights the importance of timely assessments of contaminant evolution in relation to travel time distributions and reactive processes, providing crucial insights for informed management decisions.

4. Conclusions

Examining 90 springs and groundwater-fed brooks in the southern Netherlands, we assessed their response to historical nitrate pollution and the impact of measures from the Dutch manure legislation and the EU Nitrates Directive. Nitrate concentrations from farmland leaching, derived from soil moisture monitoring programs and historical farm bookkeeping records, peaked in 1985, declined until 2010, and then stabilized. Nitrate levels at the springs, combined with tritium measurements every eight years, helped constrain the age distributions of the spring waters. An age histogram approach was applied to derive distribution-free groundwater age distributions, by convoluting precipitation inputs of tritium and historical nitrate concentrations of leachate water under farmlands for 8008 possible age distributions, finding the 50 distributions which best fitted the measured tritium and nitrate concentrations at each spring. This approach accommodated multimodal travel time distributions, particularly relevant for springs draining the dual permeability chalk aquifers in the southern region.

The study shows that farmers have reduced soil nitrogen surpluses, resulting in trend reversals at all springs, with peak concentrations and response times varying by the age distribution of outflowing water. The young fraction (water aged $<$30 years) and Mean Travel Time (MTT) were key variables in distinguishing spring responses, with values ranging from 0.18 to 1.0 and 11 to 70 years, respectively. Springs draining predominantly young water (fraction $>$0.6) had higher peak concentrations, shorter lag times, and steeper declines after trend reversal, relative to trends in springs that are dominantly fed by older groundwater. The lag between leaching and outflow peaks was best explained by the fraction of water aged $<$15 years, with longer lag times associated with smaller or absent fractions of this very young water, attributed to unsaturated zone flow delaying the onset of saturated flow contributing to spring outflow.

Despite the common notion that delayed flow through a thick unsaturated zone contributes considerably to the enduring impact of historical nitrate use, often referred to as a “nitrate time bomb” (Wang et al., 2013), our findings suggest limitations on the legacy effects regarding nitrate peak concentrations. Springs with long MTTs and less young water exhibited lower nitrate peaks, a more diluted response, and generally prolonged lag times, in contrast to springs with short MTTs. Assuming conservative transport, nitrate concentrations in all springs eventually stabilize at average leachate input levels. The sustained, continuous loading of the groundwater system leads to a long stabilization process towards the long-term average leachate inputs for those springs with delayed flows, whereas high nitrate peaks and faster stabilization occur in springs with short MTTs. In our study, springs with intermediate MTTs (30–40 years) showed slower stabilization than springs with short MTTs, yielding higher concentrations in the 2027 and 2035 forecasts.

In conclusion, by integrating measured nitrate concentrations from farmland leachate and time series data of nitrate and tritium concentrations at the springs, we modelled the age distribution and traced the evolution of tritium and nitrate over time. Our findings underscore that the nitrate legacy within groundwater systems is strongly determined by travel time distributions and thus by conservative, non-reactive subsurface transport. Trend reversals in the springs and groundwater-fed brooks appeared within 10 to 15 years post-implementation of nitrate reduction measures, even in areas with thick unsaturated zones. However, many springs draining the Zuid-Limburg loess plateaus are not expected to meet the EU Groundwater Directive's nitrate standard of 50 mg/l by 2027 due to continuous nitrate loading from high leachate concentrations between 1985 and 2020. Our study suggests that the southern chalk springs might benefit from saturated zone denitrification in part of the outflowing water, yielding potential compliance with the EU Nitrate Directive standard of 50 mg/l, but are unlikely to meet the EU Water Framework Directive or Natura2000 thresholds of respectively 10 and 18 mg NO_3/l soon, given the prolonged loading of the system at concentrations above these thresholds. The methodology employed in this study, combining nitrate and tritium time series, is promising for evaluating nitrate trends in springs and groundwater abstractions across diverse regions, aiding compliance assessments for the EU Water Framework Directive by 2027.

Acknowledgments & data policy

This research was funded by the Ministerie van Landbouw, Natuur en Voedselkwaliteit (Dutch Ministry of Agriculture, Nature and Food Quality), as part of the National Minerals Policy Monitoring Programme (Project Numbers M/350701/22 and M/350601/18) and partly through the GEOERA RESOURCE project, which received funding from the European Union's Horizon 2020 research and innovation program under grant agreement No 731166. The authors would like to thank the farmers for allowing access to their fields, the RIVM field-work team for collecting samples, and the TNO laboratory team for conducting the experiments. We would also like to thank Susanne Wuijts and Jappe Beekman of RIVM for critically reviewing the draft, and Eric Castenmiller, Andrea Kan, and Jean Hacking of the Province of Limburg for organizing the collection of the provincial datasets and making the data and metadata available. Roel Dijksma (WUR) and Birgitta Putters (WML) are thanked for delivering historical nitrate data for specific springs. Four anonymous reviewers are gratefully acknowledged for their constructive comments on the original manuscript. A summary of relevant data is available in Tables S1–S4. Moreover, the measured nitrate and sulfate data of 90 springs, the tritium and nitrate input data for the convolution models and the age distributions metrics for the base case model and the stringent denitrification model are available at Zenodo via https://doi.org/10.5281/zenodo.13256189 under license CC BY-NC-ND 4.0 (Broers et al., 2024).

CRediT authorship contribution statement

Hans Peter Broers: Writing – original draft, Visualization, Software, Resources, Methodology, Investigation, Funding acquisition, Formal analysis, Conceptualization. **Mariëlle van Vliet:** Writing – original draft, Visualization, Validation, Resources, Project administration, Methodology, Investigation, Funding acquisition, Data curation, Conceptualization. **Tano Kivits:** Writing – review & editing, Software, Methodology, Investigation, Formal analysis, Data curation. **Ronald Vernes:** Writing – review & editing, Validation, Investigation. **Timo Brussée:** Writing – review & editing, Validation, Project administration, Data curation. **Jürgen Sültenfuß:** Writing – review & editing, Validation, Resources, Formal analysis, Data curation. **Dico Fraters:** Writing – review & editing, Validation, Methodology, Funding acquisition, Conceptualization.

Declaration of generative AI and AI-assisted technologies in the writing process

During the preparation of this work the authors used ChatGPT 3.5 in order to improve readability and language. After using this tool/service, the authors reviewed and edited the content as needed and take full responsibility for the content of the publication.

Declaration of competing interest

The authors declare that they have no known competing financial interests or personal relationships that could have appeared to influence the work reported in this paper.

Data availability

Data will be made available on request.

Appendix A. Supplementary data

Supplementary data to this article can be found online at https://doi.org/10.1016/j.scitotenv.2024.175250.

References

Alikhani, J., Deinhart, A.L., Visser, A., Bibby, R.K., Purtschert, R., Moran, J.E., Esser, B. K., 2016. Nitrate vulnerability projections from Bayesian inference of multiple groundwater age tracers. J. Hydrol. 543, 167–181.

Ascott, M.J., Gooddy, D.C., Wang, L., Stuart, M.E., Lewis, M.A., Ward, R.S., Binley, A.M., 2017. Global patterns of nitrate storage in the vadose zone. Nat. Commun. 8 (1), 1416.

Bailly-Comte, V., Ladouche, B., Charlier, J.B., Hakoun, V., Maréchal, J.C., 2023. XLKarst, an excel tool for time series analysis, spring recession curve analysis and classification of karst aquifers. Hydrgeol. J. 31 (8), 2401–2415.

Böhlke, J.K., 2002. Groundwater recharge and agricultural contamination. Hydrgeol. J. 10 (1), 153–179.

Boumans, L., Fraters, D., van Drecht, G., 2008. Mapping nitrate leaching to upper groundwater in the sandy regions of The Netherlands, using conceptual knowledge. Environ. Monit. Assess. 137, 243–249.

Broers, H.P., Van der Grift, B., 2004. Regional monitoring of temporal changes in groundwater quality. J. Hydrol. 296 (1–4), 192–220.

Broers, H.P., Sültenfuß, J., Aeschbach, W., Kersting, A., Menkovich, A., de Weert, J., Castelijns, J., 2021. Paleoclimate signals and groundwater age distributions from 39 public water works in the Netherlands; insights from noble gases and carbon, hydrogen, and oxygen isotope tracers. Water Resour. Res. 57, e2020WR029058 https://doi.org/10.1029/2020WR029058.

Broers, H.P., van Vliet, M., Kivits, T., Brussée, T., Sültenfuß, J., Fraters, D., 2024. Nitrate trend reversal in Dutch dual-permeability chalk springs, evaluated by tritium-based groundwater travel time distributions [Data set]. Zenodo. https://doi.org/10.5281/zenodo.13256189.

CBS, 2023. Agricultural emissions lower than in 1995, no more decline in recent years. National Bureaus of Statistics (CBS). https://www.cbs.nl/en-gb/news/2023/09/agricultural-emissions-lower-than-in-1995-no-more-decline-in-recent-years.

CBS STATLINE, 2023. Statline Open data National Bureaus of Statistics (CBS). https://opendata.cbs.nl/statline/#/CBS/nl/dataset/80781ned/table?ts=1689505638133.

Cleveland, W.S., Devlin, S.J., 1988. Locally weighted regression: an approach to regression analysis by local fitting. J. Am. Stat. Assoc. 83 (403), 596–610.

De Mars, H., Van Dijk, G., Van der Weijden, B., Grootjans, A.P., Wołejko, L., Farr, G., Graham, J., Oosterlynck, P., Smolders, A.J., 2024. The threat of groundwater pollution for petrifying springs; defining nutrient threshold values for an endangered bryophyte-dominated habitat. Environ. Pollut. 123324.

Dessirier, B., Blicher-Mathiesen, G., Andersen, H.E., Gustafsson, B., Müller-Karulis, B., Van Meter, K., Humborg, C., 2023. A century of nitrogen dynamics in agricultural watersheds of Denmark. Environ. Res. Lett. 18 (10), 104018.

Duijvenbooden, W.V., Waegeningh, H.V., 1987. Vulnerability of Soil and Groundwater to Pollutants: International Conference Noordwijk Ann Zee, the Netherlands, March 30–April 3, 1987. TNO Committee on Hydrological Research, The Hague, pp. 2–5.
Eberts, S.M., Böhlke, J.K., Kauffman, L.J., Jurgens, B.C., 2012. Comparison of particle-tracking and lumped-parameter age-distribution models for evaluating vulnerability of production wells to contamination. Hydrgeol. J. 20 (2), 263–282.
EU Commission, 1991. Directive 91/676/EEC. Council Directive of 12 December 1991 concerning the protection of waters against pollution caused by nitrates from agricultural sources. Official Journal of European Community L 375, 1–8.
Fraters, D., Boumans, L.J., van Drecht, G., de Haan, T., de Hoop, W.D., 1998. Nitrogen monitoring in groundwater in the sandy regions of the Netherlands. Environ. Pollut. 102 (1), 479–485.
Fraters, D., Boom, G.J.F.L., Boumans, L.J.M., De Weerd, H., Wolters, M., 2017. Extraction of soil solution by drainage centrifugation - effects of centrifugal force and time of centrifugation on soil moisture recovery and solute concentration in soil moisture of loess subsoils. Environ. Monit. Assess. 189 (83) https://doi.org/10.1007/s10661-017-5788-7, 18 pages.
Fraters, B., Hooijboer, A.E.J., Vrijhoef, A., Plette, A.C.C., Van Duijnhoven, N., Rozemeijer, J.C., Gosseling, M., Daatselaar, C.H.G., Roskam, J.L., Begeman, H.A.L., 2021. Agricultural Practice and Water Quality in the Netherlands: Status (2016–2019) and Trend (1992–2019). Nitrate Report with the Results of the Monitoring of the Effects of the EU Nitrates Directive Action Programmes. National Institute for Public Health and the Environment, Bilthoven, the Netherlands (RIVM report 2020-0184.).
Fraters, D., Ros, G.H., Brussée, T., 2023. Measuring nitrate leaching in the vadose zone of loess soils—comparison of batch extraction and centrifugation. Water 15, 2709. https://doi.org/10.3390/w15152709.
Golden, H.E., Evenson, G.R., Christensen, J.R., Lane, C.R., 2023. Advancing watershed legacy nitrogen modeling to improve global water quality. Environ. Sci. Technol. 57 (7), 2691–2697.
Hansen, B., Thorling, L., Dalgaard, T., Erlandsen, M., 2010. Trend reversal of nitrate in Danish groundwater-a reflection of agricultural practices and nitrogen surpluses since 1950. Environ. Sci. Tech. 45 (1), 228–234.
Hendrix, W.P.A.M., 1985. The Groundwater of the Central Plateau in Southern Limburg (in Dutch). Report Geografische Instituut de Rijksuniversiteit Utrecht, 207p.
Hendrix, W.P.A.M., 1990. Bronnen in Zuid-Limburg (in Dutch). Natuurhistorisch Maandblad 79 (3–4), 50–62.
Hendrix, W.P.A.M., Meinardi, C.R., 2004. Bronnen en bronbeken in Zuid-Limburg, Kwaliteit van grondwater, bronwater en beekwater (in Dutch), RIVM rapport 500003003/2004. Rijksinstituut voor Volksgezondheid en Milieu, Bilthoven, The Netherlands, p. 82.
Henkens, P.L.C.M., van Keulen, H., 2001. Mineral policy in the Netherlands and nitrate policy within the European Community. Wageningen. J. Life Sci. 49, 117–134. https://doi.org/10.1016/S1573-5214(01)80002-6.
IAEA/WMO, 2018. Global Network of Isotopes in Precipitation, The GNIP Database. available at: http://www.iaea.org/water (last access: November 2018), 2018.
Jurgens, B.C., et al., 2012. TracerLPM (Version 1): An Excel® workbook for interpreting groundwater age distributions from environmental tracer data: U.S. Geological Survey Techniques and Methods Report 4-F3, 60 pp. U.S. Geological Survey, Reston, Virginia.
Jurgens, B.C., Böhlke, J.K., Kauffman, L.J., Belitz, K., Esser, B.K., 2016. A partial exponential lumped parameter model to evaluate groundwater age distributions and nitrate trends in long-screened wells. J. Hydrol. 543, 109–126.
Kaandorp, V.P., De Louw, P.G.B., van der Velde, Y., Broers, H.P., 2018. Transient groundwater travel time distributions and age-ranked storage-discharge relationships of three lowland catchments. Water Resour. Res. 54 (7), 4519–4536.
Kaandorp, V.P., Broers, H.P., Van Der Velde, Y., Rozemeijer, J., De Louw, P.G., 2021. Time lags of nitrate, chloride, and tritium in streams assessed by dynamic groundwater flow tracking in a lowland landscape. Hydrol. Earth Syst. Sci. 25 (6), 3691–3711.
Katz, B.G., Böhlke, J.K., Hornsby, H.D., 2001. Timescales for nitrate contamination of spring waters, northern Florida, USA. Chem. Geol. 179 (1–4), 167–186.
Kivits, T., Broers, H.P., Beeltje, B., van Vliet, M., Griffioen, J., 2018. Presence and fate of veterinary antibiotics in age-dated groundwater in areas with intensive livestock farming. Environ. Pollut. 241, 988–998. https://doi.org/10.1016/j.envpol.2018.05.085.
KNMI, 2020, July 14. Weather station 380 Maastricht, period 1990–2019. from. https://www.knmi.nl/nederland-nu/klimatologie/daggegevens.
Kros, H., Cals, T., Gies, E., Groenendijk, P., Lesschen, J.P., Voogd, J.C., Velthof, G., 2024. Region oriented and integrated approach to reduce emissions of nutrients and greenhouse gases from agriculture in the Netherlands. Sci. Total Environ. 909, 168501.
Kuniansky, E.L., Taylor, C.J., Williams, J.H., Paillet, F., 2023. Introduction to karst aquifers. https://gw-project.org/books/introduction-to-karst-aquifers/.
Leray, S., Engdahl, N.B., Massoudieh, A., Bresciani, E., McCallum, J., 2016. Residence time distributions for hydrologic systems: mechanistic foundations and steady-state analytical solutions. J. Hydrol. 543, 67–87.
van Loon, A.H., Fraters, D., 2016. De gevolgen van mestgebruik voor drinkwaterwinning. In: KWR rapport 2016.023.
Mak, W., Bakker, P., Frapporti, G., 1999. Evaluatie Provinciaal meetnet grondwaterkwaliteit Limburg en Bodemvochtmeetnet Nitraat Mergelland. IWACO, report 3361410.
Maloszewski, P., Zuber, A., 1982. Determining the turnover time of groundwater systems with the aid of environmental tracers. 1. Models and their applicability. J. Hydrol. 57 (3–4), 207–231.
Maloszewski, P., Zuber, A., 1993. Principles and practice of calibration and validation of mathematical models for the interpretation of environmental tracer data in aquifers. Adv. Water Resour. 16 (3), 173.
Maloszewski, P., Zuber, A., 1998. A general lumped parameter model for the interpretation of tracer data and transit time calculation in hydrologic systems – comments. J. Hydrol. 204 (1–4), 297–300.
Maréchal, J.C., Bailly-Comte, V., Hickey, C., Maurice, L., Stroj, A., Bunting, S.Y., Charlier, J.B., Hakoun, V., Herms, I., Krystofova, E., Pardo-Igúzquiza, E., Persa, G., Shubert, D., Skopljak, F., Szucs, A., Urbanc, J., Van Vliet, M.E., Vernes, R.W., 2021. Karst aquifer typology tool. Deliverable 5.3. Chaka Project. GeoERA RESOURCE Project. https://repository.europe-geology.eu/egdidocs/resource/geoera+resource+chaka+deliverable+53+karst+typolo.pdf.
Massoudieh, A., Visser, A., Sharifi, S., Broers, H.P., 2014. A Bayesian modeling approach for estimation of a shape-free groundwater age distribution using multiple tracers. Appl. Geochem. 50, 252–264.
McCallum, J.L., Cook, P.G., Dogramaci, S., Purtschert, R., Simmons, C.T., Burk, L., 2017. Identifying modern and historic recharge events from tracer-derived groundwater age distributions. Water Resour. Res. 53 (2), 1039–1056.
Meinardi, C.R., 1994. Groundwater recharge and travel times in the sandy regions of the Netherlands.PhD Thesis VU Amsterdam.R VM report;no. 715501004.
Mendizabal, I., Stuyfzand, P.J., 2011. Quantifying the vulnerability of well fields towards anthropogenic pollution: the Netherlands as an example. J. Hydrol. 398, 260–276.
Mendizabal, I., Baggelaar, P.K., Stuyfzand, P.J., 2012. Hydrochemical trends for public supply well fields in the Netherlands (1898–2008), natural backgrounds and upscaling to groundwater bodies. J. Hydrol. 450, 279–292.
Mull, D.S., Liebermann, T.D., Smoot, J.L., Woosley, Jr, L.H., Mikulak, R.J., 1988. Application of dye-tracing techniques for determining solute-transport chrachteristics of groundwater in kart terranes. US-EPA/ USGS, report EPA904/ 6–88-001.
Oenema, O., Boers, P.C.M., Van Eerdt, M.M., Fraters, B., Van der Meer, H.G., Roest, C.W.J., Willems, W.J., 1998. Leaching of nitrate from agriculture to groundwater: the effect of policies and measures in the Netherlands. Environ. Pollut. 102 (1), 471–478.
van Ommen, H.C., 1986. Influence of diffuse sources of contamination on the quality of outflowing groundwater including non-equilibrium adsorption and decomposition. J. Hydrol. 88, 79–95. https://doi.org/10.1016/0022-1694(86)90198-8.
Osenbrück, K., et al., 2006. Timescales and development of groundwater pollution by nitrate in drinking water wells of the Jahna-Aue, Saxonia, Germany. Water Resources Research 42 (12), W12416.
Post, P.M., Hogerwerf, L., Bokkers, E.A., Baumann, B., Fischer, P., Rutledge-Jonker, S., de Boer, I.J., 2020. Effects of Dutch livestock production on human health and the environment. Sci. Total Environ. 737, 139702.
Provincie Limburg, 2021. Provinciaal Waterprogramma 2022–2027. https://www.limburg.nl/publish/pages/979/2201_071_provinciaal_waterprogramma_2022-2027.pdf.
Quinlan, James F., Ewers, Ralph O., 1985. Ground Water Flow in Limestone Terranes: Strategy Rationale and Procedure for Reliable, Efficient Monitoring of Ground Water Quality in Karst Area, in Proceedings of the Fifth National Symposium and Exposition on Aquifer Restoration and Ground Water Monitoring: Worthington, Ohio, National Water Well Association, pp. 197–234.
Rädle, V., Kersting, A., Schmidt, M., Ringena, L., Robertz, J., Aeschbach, W., Müller, T., 2022. Multi-tracer groundwater dating in southern Oman using Bayesian modeling. Water Resour. Res. 58 (6), e2021WR031776.
Ros, G.H., 2014. Comparison monitoring protocols for nitrate in soil moisture (in Dutch) Kennisbundeling nitraatmeting bodemvocht lössgronden. Vergelijking meetprotocollen WML, LMM en BVM. Nutriënten Management Instituut NMI B.V, report 1559.N.14.
Sarrazin, F.J., Kumar, R., Basu, N.B., Musolff, A., Weber, M., Van Meter, K.J., Attinger, S., 2022. Characterizing catchment-scale nitrogen legacies and constraining their uncertainties. Water Resour. Res. 58 (4), e2021WR031587.
Schipper, P.N.M., Vissers, M.J.M., van der Linden, A.A., 2008. Pesticides in groundwater and drinking water wells: overview of the situation in the Netherlands. Water Sci. Technol. 57 (8), 1277–1286.
Sjerps, R.M.A., Kooij, P.J.F., van Loon, A., van Wezel, A.P., 2019. Occurence of pesticides in Dutch drinking water sources. Chemosphere 235, 510–518.
Solder, J.E., Stolp, B.J., Heilweil, V.M., Susong, D.D., 2016. Characterization of mean transit time at large springs in the Upper Colorado River Basin, USA: a tool for assessing groundwater discharge vulnerability. Hydrgeol. J. 24 (8), 2017.
Spijker, J., Fraters, D., Vrijhoef, A., 2021. A machine learning based modelling framework to predict nitrate leaching from agricultural soils across the Netherlands. Environ. Res. Commun. 3, 45002.
Stolp, B.J., Solomon, D.K., Suckow, A., Vitvar, T., Rank, D., Aggarwal, P.K., Han, L.F., 2010. Age dating base flow at springs and gaining streams using helium-3 and tritium: Fischa-Dagnitz system, southern Vienna Basin, Austria. Water Resources Research 46 (7).
Suckow, A., 2012. Lumped Parameter Modelling of Age Distributions using up to two Parallel Black Boxes (Manual, Version 2.1).
Suckow, A., 2014. The age of groundwater–Definitions, models and why we do not need this term. Appl. Geochem. 50, 222–230.
Suckow, A., Gerber, C., Kralik, M., Sültenfuss, J., Purtschert, R., 2013, April. The Fischa-Dagnitz spring, southern Vienna Basin: a multi tracer time series study re-assessing earlier conceptual assumptions. In: EGU General Assembly Conference Abstracts (pp. EGU2013-6610).
Sültenfuß, J., Roether, W., Rhein, M., 2009. The Bremen mass spectrometric facility for the measurement of helium isotopes, neon, and tritium in water. Isotopes Environ. Health Stud. 45 (2), 83–95. https://doi.org/10.1080/10256010902871929.

Tesoriero, A.J., Burow, K.R., Frans, L.M., Haynes, J.V., Hobza, C.M., Lindsey, B.D., Solder, J.E., 2019. Using age tracers and decadal sampling to discern trends in nitrate, arsenic, and uranium in groundwater beneath irrigated cropland. Environ. Sci. Technol. 53 (24), 14152–14164.

Teuling, A.J., 2001. Een studie naar de afvoerkarakteristieken van de Sint-Brigidabron en de invloed van tektoniek op de hydrogeologie van het Nederlandse deel van het stroomgebied van de Noor met behulp van MODFLOW (Publication No. HG 187) [Master's thesis, Wageningen University]. Wageningen University, Wageningen, the Netherlands.

Tiktak, A., De Nie, D., Van Der Linden, T., Kruijne, R., 2002. Modelling the leaching and drainage of pesticides in the Netherlands: the GeoPEARL model. Agronomie 22 (4), 373–387.

TNO-GSN, 2020a. Gulpen Formation. In: Stratigraphic Nomenclature of the Netherlands, TNO – Geological Survey of the Netherlands. Accessed on 22-07-2020 from. http://www.dinoloket.nl/en/stratigraphic-nomenclature/gulpen-formation.

TNO-GSN, 2020b. Maastricht Formation. In: Stratigraphic Nomenclature of the Netherlands, TNO – Geological Survey of the Netherlands. Accessed on 22-07-2020 from. http://www.dinoloket.nl/en/stratigraphic-nomenclature/maastricht-formation.

Van Boekel, E.M.P.M., Groenendijk, P., Kros, J., Renaud, L.V., Voogd, J.C., Ros, G.H., van Dijk, W., 2021. Effects of measures in the 7th action programme for the Nitrates Directive. Effecten van maatregelen in het Zevende Actieprogramma Nitraatrichtlijn: Milieueffectrapportage op planniveau. In Dutch, with English summary. Report No. 3108, /Wageningen Environmental Research. https://doi.org/10.18174/553651.

Van den Brink, C., Zaadnoordijk, W.J., van der Grift, B., de Ruiter, Griffioen, J., 2008. Using a groundwater quality negotiation support system to change land-use management near a drinking-water abstraction in the Netherlands. J. Hydrol. 350 (3–4), 339–356.

Van der Velde, Y., De Rooij, G.H., Rozemeijer, J.C., Van Geer, F.C., Broers, H.P., 2010. Nitrate response of a lowland catchment: on the relation between stream concentration and travel time distribution dynamics. Water Resour. Res. 46 (11).

Van Duijnen, R., Van Leeuwen, T.C., Hoogeveen, M.W., 2021. Minerals policy monitoring programme report 2015–2018 methods and procedures. In: National Institute for Public Health and the Environment, Bilthoven, the Netherlands, RIVM report 2020–0163.

Van Grinsven, H.J.M., Ten Berge, H.F.M., Dalgaard, T., Fraters, B., Durand, P., Hart, A., Willems, W.J., 2012. Management, regulation and environmental impacts of nitrogen fertilization in northwestern Europe under the nitrates directive; a benchmark study. Biogeosciences 9 (12), 5143–5160.

Van Grinsven, Tiktak, A., Rougoor, C.W., 2016. Evaluation of the Dutch implementation of the nitrates directive, the water framework directive and the national emission ceilings directive. NJAS-Wagening. J. Life Sci. 78, 69–84.

Van Lanen, H.A.J., Heijnen, M., De Jong, T., Van Der Weerd, B., 1993. Nitrate concentrations in the Gulp catchment: some spatial and temporal considerations. Acta geológica hispánica 65–73.

Van Maanen, J.M.S., De Vaan, M.A.J., Veldstra, A.W.F., Hendrix, W.P.A.M., 2001. Pesticides and nitrate in groundwater and rainwater in the province of Limburg in the Netherlands. Environ. Monit. Assess. 72, 95–114.

Van Meter, K.J., Basu, N.B., Veenstra, J.J., Burras, C.L., 2016. The nitrogen legacy: emerging evidence of nitrogen accumulation in anthropogenic landscapes. Environ. Res. Lett. 11 (3), 035014.

Van Rooijen, P., 1993. The Netherlands. In: Downing, R.A., Price, M., Jones, G.P. (Eds.), The Hydrogeology of the Chalk of North-West Europe. Clarendon Press, Oxford, United Kingdom, pp. 170–185.

Vernes, R.W., Hummelman, H.J., Menkovic, A., Reindersma, R., 2018. Estimating the hydraulic conductivity and transmissivity of the chalk aquifer in South-Limburg, the Netherlands. [Conference session]. The Hydrogeology of the Chalk, The Geological Society, Burlington House, London, United Kingdom. 25 April 2018.

Visser, A., Broers, H.P., Van der Grift, B., Bierkens, M.F.P., 2007. Demonstrating trend reversal of groundwater quality in relation to time of recharge determined by 3H/3He. Environ. Pollut. 148 (3), 797–807.

Visser, A., Broers, H.P., Heerdink, R., Bierkens, F.P., 2009. Trends in pollutant concentrations in relation to time of recharge and reactive transport at the groundwater body scale. J. Hydrol. (3-4), 427–439.

Visser, A., Broers, H.P., Purtschert, R., Sültenfuß, J., de Jonge, M., 2013. Groundwater age distributions at a public drinking water supply well field derived from multiple age tracers (85Kr, 3H/3He, and 39Ar). Water Resour. Res. 49 (11), 7778–7796.

Visser, A., Moran, J.E., Hillegonds, D., Singleton, M.J., Kulongoski, J.T., Belitz, K., Esser, B.K., 2016. Geostatistical analysis of tritium, groundwater age and other noble gas derived parameters in California. Water Res. 91, 314–330.

Vogel, J.C., 1967. Investigation of groundwater flow with radiocarbon., paper presented at IAEA Symposium on Isotopes in Hydrology, 14–18 November 1966, IAEA, Vienna, Austria.

Wang, L., Butcher, A.S., Stuart, M.E., Gooddy, D.C., Bloomfield, J.P., 2013. The nitrate time bomb: a numerical way to investigate nitrate storage and lag time in the unsaturated zone. Environ. Geochem. Health 35, 667–681.

Worthington, S.R., Ford, D.C., 2009. Self-organized permeability in carbonate aquifers. Groundwater 47 (3), 326–336.

Zhang, Y.-C., et al., 2009. Denitrification coupled to pyrite oxidation and changes in groundwater quality in a shallow sandy aquifer. Geochim Cosmochim Ac 73 (22), 6716–6726.

Zhang, Y.C., Slomp, C.P., Broers, H.P., Bostick, B., Passier, H.F., Böttcher, M.E., Omoregie, E.O., Lloyd, J.R., Polya, D.A., Van Cappellen, P., 2012. Isotopic and microbiological signatures of pyrite-driven denitrification in a sandy aquifer. Chem. Geol. 300, 123–132.